ON-SITE DIAGNOSTIC TESTING OF MOSA USING THE NEUTRAL CURRENT METHOD

By

CUIJIAO MA

A Thesis

Submitted to the Faculty of Graduate Studies

In Partial Fulfillment of the Requirements

For the Degree of

MASTER OF SCIENCE

Department of Electrical and Computer Engineering
University of Manitoba
Winnipeg, Manitoba

THE UNIVERSITY OF MANITOBA

FACULTY OF GRADUATE STUDIES

*****

COPYRIGHT PERMISSION

On-Site Diagnostic Testing of MOSA Using the Neutral Current Method

BY

Cuijiao Ma

A Thesis/Practicum submitted to the Faculty of Graduate Studies of The University of Manitoba in partial fulfillment of the requirement of the degree

Of

Master of Science

ACKNOWLEDGEMENTS

I would like to express my profound gratitude and appreciation to my advisor, Dr. M. R. Raghuveer, for his invaluable enthusiasm, encouragement, guidance and support in this study. The completion of this thesis owes to his rigorous scientific approach and strict demand on the research.

I am indebted to Prof. Yuchang Qiu (Xi'an Jiaotong University, China) for his encouragement to do higher studies and arranging the opportunity for me to do so.

Funding from Manitoba Hydro and National Science and Engineering Research Council, Canada is gratefully acknowledged.

I appreciate and acknowledge Mr. W.McDermid, P. Eng, for his kind action as liaison officer and project consultant.

I would also like to thank Mr. John Kendall, technologist of high voltage laboratory of University of Manitoba, for his technical help on numerous occasions during this study.

Finally, my appreciation should be expressed to my husband for being there when I need him.

ABSTRACT

With the passage of time, a Metal Oxide Surge Arrester (MOSA) in service may exhibit ageing which manifests itself in an increased component of resistive current with accompanying increase in the third harmonic component. Diagnostic methods based on measurement of these components have been found to lend themselves to on-site diagnostics and are very popular.

In this research, a simpler on-site MOSA diagnostic testing technique based on the measurement of neutral current is considered. A program in LabVIEW language is developed for phase identification of the aged element or elements. The instrumentation associated with this method will be portable and the method may be used by non-specialists to quickly assess the condition of arresters and decide whether or not a more detailed investigation is required. It is shown that the neutral current based arrester diagnostic technique, in contrast to other methods based on harmonic analysis, is particularly insensitive to the influence of harmonics present in the system voltage. The effects of inter-phase interference and unbalanced phase voltages are also studied.

TABLE OF CONTENTS

LIST OF SYMBOLS

C	Capacitance of metal oxide valve element
C_{ab}	Stray capacitance between phases A and B
C_{ac}	Stray capacitance between phases A and C
G	Constant corresponding to ωC
I_C, i_c	Capacitive current of MOSA
i_{c1}	Fundamental capacitive current
I_{min}	Minimum peak value of the three peaks of the neutral current
I_n	Neutral current
I_1, I_2, I_3	Three peak values of the neutral current
I_{BM}	Benchmark value
I_R, i_r	Resistive current of MOSA
I_{r3}	3rd resistive harmonic current
i_t,	Total current of MOSA
I_0	RMS value of the neutral current
k_1, k_2, k_3	Three waveshape factors of the neutral current
L	Inductance of metal oxide disc
R	Nonlinear resistance of metal oxide valve element
R_i	Resistance of the granular layers
R_z	Resistance of ZnO grains
V, v	Voltage across the arrester
V_a, V_b, V_c	Phase to ground voltage of phases A, B and C
V_N	Rated voltage of MOSA
v_n	nth harmonic voltage
v_{n0}	nth harmonic voltage phase shifted forward by 90°

v_{s0}	System voltage phase shifted forward by 90°
v_{1s0}	Fundamental component of v_{s0}
V_3	3rd harmonic voltage
V_5	5th harmonic voltage
Φ_3	Phase angle of 3rd harmonic voltage
Φ_5	Phase angle of 5th harmonic voltage
ρ	Resistivity
ε_r	Relative dielectric constant

LIST OF FIGURES

LIST OF TABLES

CHAPTER 1

Introduction

Overvoltages in electrical power systems caused by lightning events or internal switching operations can reach dangerous amplitudes for high voltage apparatus. To protect transmission and distribution equipment from overvoltages, and to improve economic and reliable operation, surge arresters are applied in almost all types of electrical power networks and play a vital role in electrical power system overvoltage protection [1].

Metal oxide surge arresters (MOSA), developed in the late 1970s, have nowadays replaced the traditional silicon carbide (SiC) arresters for overvoltage protection, offering significant advantages in terms of protective performance, energy capability and reliability [2].

1.1 General Characteristic of a Metal Oxide Valve Element

MOSA valve elements primarily consist of Zinc Oxide (ZnO) together with small

amounts of additive materials such as Oxides of Bismuth, Cobalt, Manganese and Antimony to produce desired characteristics. The valve elements are disc-shaped with their cross sectional area approximately proportional to the energy the disk must dissipate in a high energy operation, and the length approximately proportional to the voltage rating assigned to the disk [3]. The microstructure of the metal oxide material composite is that the low resistive ZnO grains are surrounded and separated by a granular layer, which is a high resistive oxide. Metal oxide surge arresters have extremely non-linear resistive characteristics. Fig. 1.1 shows the resistive voltage-current characteristics of a metal oxide (MO) disc.

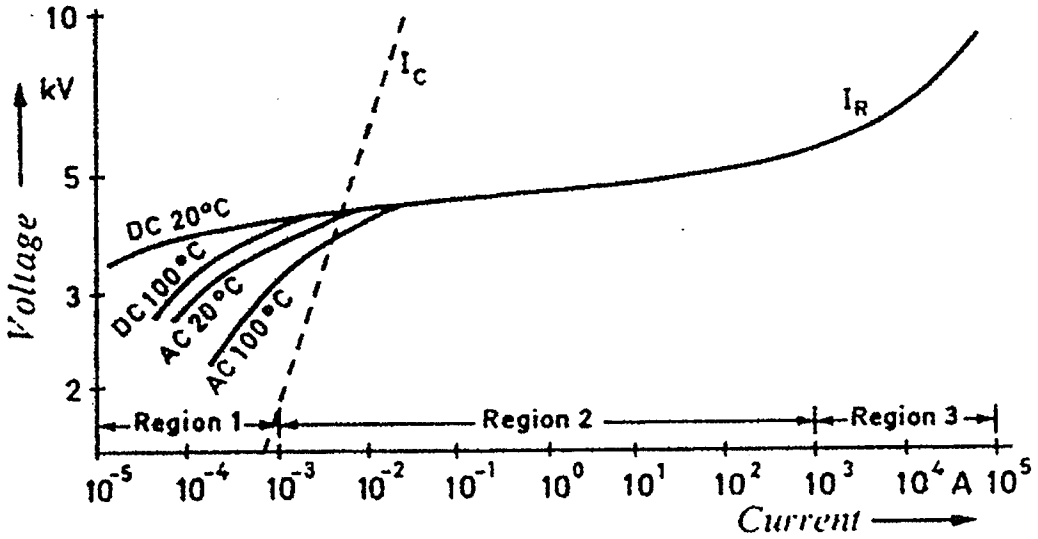

Fig. 1.1 Typical voltage current characteristics of a metal oxide disc (80 mm diameter, 20 mm height) [4]

As shown in Fig.1.1, the voltage-current characteristic of the MOSA valve disc

offers the degree of non-linearity necessary to fulfill the mutually contradicting requirement of a low protection level at high current values and a low current, i.e. a low power dissipation, at the system operating voltage. Unlike SiC arresters, metal oxide surge arresters can be connected to the system without series spark-gaps because of the high nonlinearity of the voltage-current characteristic. This feature together with its fast transient response and large energy capability has allowed the replacement of SiC arresters with metal oxide arresters.

Based on the conduction mechanism of the microstructure, the resistive voltage-current characteristics of the MOSA in Fig. 1.1 may be divided into three regions: the low electric field region (region 1), the medium electric field region (region 2) and the high electric field region (region 3). In the first conduction stage, at low electric fields, the resistive current has poor non-linear characteristics, and depends not only on the applied voltage, but also on the valve element temperature. A negative temperature coefficient is exhibited in the low-current operating region. The conduction mechanism of MOSA in the region 1 is explained by means of energy barriers in the granular layers [4]. The barriers prevent electrons from moving from one layer to another; but the electric field can lower these barriers and cause small quantities of electrons to pass. This current which arises due to Schottky emission is the resistive current. A higher temperature causes higher electron energy and results in more electrons to pass over barriers.

In the medium electric field region, the conduction mechanism of the metal oxide

valve element can be explained by the tunnel effect. In the high electric field region, the voltage drop at the barrier due to the tunnel effect is small and the voltage drop across the resistance of the ZnO grains dominates. The current then gradually approaches the linear relation with the voltage.

In order to keep the power dissipation in a metal oxide surge arrester due to the system operating voltage small, the continuous operating voltage (MCOV) of the MOSA has to be chosen in the low electric field region. The protective characteristics of the arrester are determined by the voltage-current characteristic in the medium and high electric field regions. In these regions the influences of temperature and capacitances have disappeared and the deviation from the linear voltage distribution along the arrester is only determined by the dispersion of the resistive voltage-current characteristic [4].

The nonlinear voltage-current characteristic of a MOSA valve disc in the operating region 1 is generally represented by the equivalent circuit shown in Fig. 1.2 [4]. The resistor R_i in Fig.1.2 represents the non-linear resistance of the granular layers, where the resistivity ρ changes from 10^8 Ωm for low electric field stress to just below 0.01 Ωm for high stress. The equivalent capacitor C represents the capacitance between the granular layers with a relative dielectric constant between 500 and 1200 depending on the manufacturing process. R_z is the resistance of the ZnO grains with a resistivity of about 0.01 Ωm. To account for rate-of-rise effects, an inductor is included as shown in Fig. 1.2. The inductance L is determined by the geometry of the current flow path.

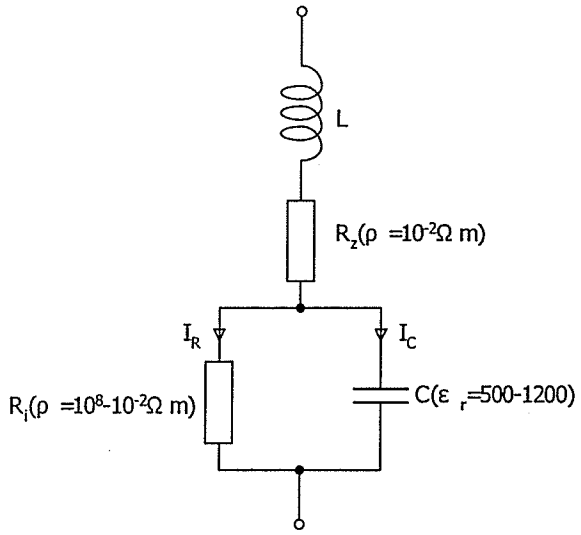

Fig. 1.2 Equivalent circuit of a MOSA valve disc [4]

This thesis focuses on the study of arrester characteristics in region 1 as shown in Fig. 1.1. In region 1, $R_z << R_i$ and inductance L may be neglected. Therefore, in the continuous operating voltage region, the metal oxide valve element may be modeled as a nonlinear resistor with a linear capacitive element in parallel.

1.2 Deterioration of MOSA

Deterioration of metal oxide surge arresters in service can be grouped into three basic types: i) deterioration under the influence of operating voltage, ii) deterioration caused by impulse currents and iii) deterioration due to chemical reactions with the surroundings [5].

i) The increase of arrester current under continuous operating voltage stress was evident for arresters of the first generation. Extensive research and development

efforts undertaken by manufacturers has resulted in modern state-of-the-art arresters which exhibit a constant or decreasing arrester current, resulting in a stable service behavior under continuous operating voltages [5].

ii) Discharge currents caused by overvoltages may lead to a change of the voltage-current characteristics or even a destruction of the arrester. During impulse stress the electrical field strength at the grain boundary of the ZnO ceramic material causes an ion-migration mainly of oxygen-ions, resulting in increased magnitude of resistive current flow at operating voltage. A high transient voltage or sustained voltage, hence a high current stress on MOSA, will cause the degradation of MOSA. High current through MOSA results in an excessive local current density through the granular layers, and this may partially destroy them.

iii) This type of degradation may occur due to internal partial discharges, possible moisture ingress, uneven heating and solar irradiation. In [5] it is mentioned that oxygen depletion of the gaseous atmosphere inside the MOSA housing will occur due to internal partial discharges. The oxygen is non-reversibly reduced out off the rim, leading to a decreased height of the potential barrier at the grain boundaries. This result in an overall symmetrical increase of the arrester current.

Moisture inside the arrester housing fills intergranular spaces and it is a very important agent which is responsible for an increase in the arrester currents. In [6]

it is reported that extracting the water from the arrester housing results in full recovery of the conducting properties of the arrester.

Uneven heating and irradiation also degrades MOSA. A simple example of these effects is due to the heat from the sun. In service, a MOSA will not be evenly heated; the heating effect also varies from season to season. This will cause the current density to be nonuniform [7].

Thus, with the passage of time, a MOSA may exhibit ageing. The aged MOSA manifests itself in an increased component of resistive current and its harmonic components especially the 3rd harmonic component. A serious consequence of this increased resistive current is that the energy absorption capability decreases which in turn may lead to thermal runaway and cause failure of MOSA. Therefore, it is very important to periodically check the condition of MOSA in service to ensure that its operating characteristics are acceptable.

1.3 Brief Review of Existing On-Site Diagnostic Testing Techniques

In order to ascertain the condition of a metal oxide surge arrester, a number of diagnostic methods have been proposed. Some of these techniques are based on the measurement of radio interference, partial discharge and emitted electromagnetic radiation. However, these methods may not detect the real operating condition of MOSA because of interference from other sources on-site.

On the other hand, diagnostic techniques based directly on the measurement of arrester current have offered the most promise. These methods which are currently used for on-site diagnostics include: measurement of the total arrester current, the resistive current, higher order harmonic currents in the resistive current and the neutral current method.

Measurement of the temperature of the metal oxide insert of an arrester is another widely used diagnostic method.

1.3.1 Total Arrester Current Method

It is well known that the degradation of a MOSA results in the increase of resistive current and consequent increase of the total arrester current. Thus, it is possible to assess the state of a MOSA by measuring the arrester current.

The total arrester current, i_t, is the sum of the current flowing through the non-linear resistor block (resistive current i_r) and the current flowing through the capacitor block (capacitive current i_c). Measurement of the total arrester current is commonly implemented by means of a permanently inserted milliampere meter in the ground connection of the arrester. Either the average of the rectified current is measured, or the average and peak level of the total current are measured by a portable instrument [8].

Experience indicates that this method has a very low sensitivity and is inadequate for determining the condition of a MOSA [8] because in the operating voltage region the

value of I_R is in range of 100 μA while the capacitive component I_C is about 1mA. According to operating experience, an obvious change in the reading of the milliampere meter will be noticed only if moisture ingress is very serious or the MOSA has aged considerably.

1.3.2 Resistive Current Method

Measurement of the resistive current is one of the best ways to determine the MOSA service behavior or the degree of degradation since it allows an immediate comparison with the expected level of resistive current at the prevailing operating condition. To obtain the resistive component of the total arrester current, a compensation method may be used to eliminate the capacitive component.

In the laboratory, in order to obtain the resistive current, one needs to use a current probe and a voltage transformer or divider having a negligible phase shift to provide the phase-correct voltage signal which may be used for elimination of the capacitive component [5].

In an AC system it is difficult to obtain the voltage signal. The authors of [5] use a technique which assumes that the phase shift between i_r and i_c (presumably between the peak of the non sinusoidal resistive current and the peak of the sinusoidal capacitive current) does not change with ageing of the valve element. The phase shift is determined in the laboratory using a compensation technique and is found to lie between 77° to 87°

for different types of arresters. The authors also assume that the capacitance of the arrester does not change with ageing.

In the field a sinusoidal signal is generated which represents the capacitive current. The resistive current is obtained by eliminating the capacitive component. Presumably the magnitude and positioning of the generated signal is changed and iterated until the correct phase shift is obtained. Thus the resistive current is obtained. This approach can be used for on-line diagnostics or monitoring.

The errors associated with the resistive current method are due to inter-phase interference and harmonic voltages [7].

1.3.3 Method Based on the Third Harmonic Content of Arrester Current

The current of a metal oxide valve element stressed with sinusoidal voltage contains a fundamental harmonic component and higher order harmonics due to its non-linear resistance. Particularly, the amplitude of the 3rd harmonic depends on the degree of nonlinearity. Therefore, the 3rd harmonic analysis can be used for diagnostics. Considerable measuring errors may occur if harmonics are present in the system voltage [8], [9].

A method developed by Swedish and Norwegian researchers [10] employs a field probe which allows compensation for the harmonic currents generated by the harmonics in the voltage. However, this method has inherent errors associated with probe placement

and assumption of a constant field factor [7]. Moisture ingress can not be detected by the 3rd harmonic analysis [5]. It is also mentioned in [5] that if an arrester is degraded by oxygen reduction, the differential steepness of the V-I-characteristics does not change. This implies that there is no change in the percent content of the third harmonic.

1.3.4 Measurement of Valve Element Temperature

The temperature of a metal oxide valve element of an arrester is the resulting effect of all influences, such as energy absorption due to impulse or temporary overvoltages, power loss increased by electrical ageing or moisture ingress. Therefore, the temperature of the MO column can be measured and used as a criterion to assess whether the arrester is working in a thermally stable condition or not.

Different methods for measuring the valve element temperature inside the arrester housing are known, mostly using an optical fiber to carry the temperature information to the receiver. Recently a new measuring system was developed [11], which allows a remote measurement of the temperature by passive sensors directly within the MO column. This system gives the possibility to realize an overall monitoring of arresters. The use of infrared imaging has been successfully used by utility to detect temperature variation or hot spots.

1.3.5 Neutral Current Method

A much simpler method, which is based on measurement of the neutral current, was

suggested by a discusser in the closure to [10]. In this method the three arrester currents are passed through a common shunt. Since the three capacitive currents will nearly sum to zero, the measured current will primarily be the sum of the resistive components. As the phase voltages are displaced by 120 degrees the resultant total current is of a rather uniform third harmonic with some fundamental component present due to stray effects. The discusser suggests that since it is extremely unlikely that all three arresters will "go bad" at the same time the current of the defective arrester will register as an increase in the appropriate third half cycle. If an arrester in one phase ages it will result in an increase in one of the peaks of the third harmonic wave shape in neutral current. This peak repeats every two cycles at third harmonic frequency. In order for this method to be used as a diagnostic technique it is necessary to identify the phase in which the aged MOSA is located. Therefore, some modifications need to be introduced.

Experiments carried out in this thesis study show that the neutral current method can be used as a diagnostic technique to identify the phase in which the aged MOSA is located. The application of the neutral current method is investigated in Chapter2, and the errors associated with this method are discussed in Chapter3.

1.4 Scope of the Present Investigation

In this thesis on-site diagnostic testing of MOSA using the neutral current method is investigated by means of laboratory experiments. A program for phase identification of

the aged element or elements has been developed in LabVIEW language. The results of the diagnostic testing technique obtained by using a laboratory setup are reported. The influence due to inter-phase interference is experimentally investigated. The errors associated with the method due to the presence of harmonics in the system voltage and the effects of unbalanced voltage are evaluated by simulation using PSCAD/EMTDC^{+}.

CHAPTER 2

Investigation of the Neutral Current Method for On-Site Diagnostic Testing of MOSA

In this chapter, the neutral current method for on-site diagnostic testing of MOSA is examined. To investigate the neutral current method, it is necessary to use MOSA valve elements whose voltage-current characteristics are known. Therefore, the v-i_r characteristics of several MOSA valve elements were obtained by application of the compensation technique. Polynomial representations of the simplified v-i_r characteristics were also obtained. Finally, a computer program was developed to enable phase identification of aged element or elements by using the neutral current method.

2.1 Investigation of the v-i_r Characteristics of MOSA

In order to investigate the on-site diagnostic techniques, it is necessary to know the v-i_r characteristics of MOSA valve elements used in experiments. The derivation of v-i_r characteristics requires experimental data and use of a computation program to implement a numerical technique.

2.1.1 Experimental Setup to Record Applied Voltage and Arrester Current

The experimental setup is shown in Fig. 2.1. The shunt is a non-inductive resistor with resistance value of 10 kΩ. The resistive divider provided by a high voltage probe (Tektronix Passive High Voltage Probe model #P6015A) has a ratio of 1000:1 (100 MΩ/10 kΩ). The total current through the valve element is obtained by measuring the voltage across the shunt and the applied voltage is measured by the high voltage probe. These two signals are captured using a Tektronix digital storage oscilloscope model #TEK TDS 3054.

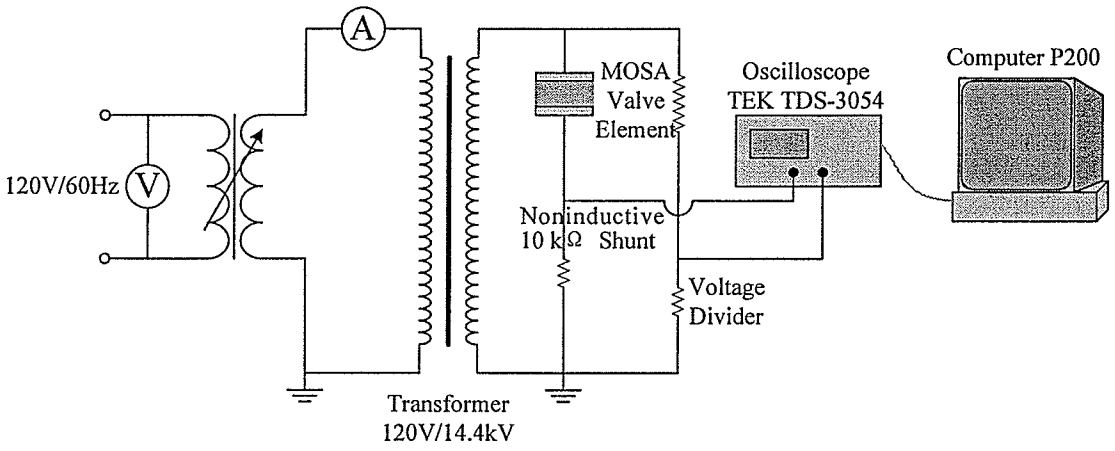

Fig. 2.1 Single phase laboratory setup to obtain arrester characteristics

Up to seventeen MO valve elements of length 44 mm and diameter 76 mm numbered #1, #2, #3... #17 were used in the single phase setup as shown in Fig. 2.1 to measure the applied voltage and the total valve element current over the voltage range 1kV to approximately 8kV (peak value). The test results are listed in Table 2.1. These results were used to categorize the condition of the valve elements as either unaged, aged or very aged.

Table 2.1 Test data of MOSA valve elements used in experiments

V.E: Valve Element, V, I are peak values and I is the total arrester current.

		Test #1	Test #2	Test #3	Test #4	Test #5	Test #6	Test #7	Test #8
V.E #1	V(kV)	1.00	2.02	3.00	4.02	5.04	6.00	7.04	8.00
	I(mA)	0.256	0.496	0.696	0.940	1.14	1.68	1.88	2.02
V.E #2	V(kV)	1.01	2.01	3.00	4.02	5.04	6.00	7.02	8.00
	I(mA)	0.248	0.432	0.672	0.880	1.04	1.58	1.76	2.02
V.E #3	V(kV)	1.00	2.01	3.00	4.00	4.98	6.00	7.02	8.00
	I(mA)	0.248	0.456	0.688	0.880	1.08	1.62	1.76	1.98
V.E #4	V(kV)	1.00	2.02	3.01	4.00	4.96	6.02	7.02	8.00
	I(mA)	0.288	0.584	0.900	1.120	1.36	1.72	1.92	2.32
V.E #5	V(kV)	1.00	2.00	3.04	3.98	5.04	6.00	6.98	--
	I(mA)	0.272	0.552	0.860	1.10	1.36	2.76	6.08	--
V.E #6	V(kV)	1.01	2.00	3.00	4.00	5.02	6.00	7.00	8.00
	I(mA)	0.304	0.576	0.880	1.10	1.340	1.64	1.86	2.26
V.E #7	V(kV)	1.00	2.00	3.00	4.00	5.02	6.00	7.02	8.00
	I(mA)	0.288	0.560	0.840	1.06	1.34	1.58	1.80	2.54
V.E #8	V(kV)	0.98	1.94	2.96	4.00	4.96	6.00	6.98	8.00
	I(mA)	0.264	0.544	0.840	1.06	1.28	1.56	1.76	1.96
V.E #9	V(kV)	0.96	1.98	3.00	4.00	4.98	6.00	6.90	7.98
	I(mA)	0.256	0.552	0.820	1.04	1.28	1.56	1.68	1.96
V.E #10	V(kV)	1.00	1.98	3.00	4.02	4.94	6.00	7.02	8.00
	I(mA)	0.264	0.560	0.860	1.06	1.28	1.56	1.76	2.04
V.E #11	V(kV)	1.00	1.98	3.02	4.00	4.96	6.00	7.00	7.96
	I(mA)	0.272	0.570	0.840	1.06	1.28	1.56	1.76	1.96
V.E #12	V(kV)	1.00	1.96	3.00	3.96	4.92	6.00	6.96	--
	I(mA)	0.279	0.584	0.880	1.14	1.38	2.16	7.74	--
V.E #13	V(kV)	0.96	1.94	3.00	4.00	5.02	6.00	7.00	7.94
	I(mA)	0.256	0.536	0.860	1.04	1.30	1.56	1.76	1.96
V.E #14	V(kV)	0.98	1.96	2.96	3.94	4.96	6.00	7.04	8.00
	I(mA)	0.272	0.560	0.840	1.04	1.28	1.56	1.82	2.00
V.E #15	V(kV)	0.96	1.94	2.96	3.94	4.90	6.04	7.02	7.96
	I(mA)	0.260	0.539	0.820	1.04	1.28	1.56	1.76	2.00
V.E #16	V(kV)	0.96	1.96	2.96	4.00	5.00	6.02	7.02	7.98
	I(mA)	0.264	0.552	0.840	1.06	1.30	1.56	1.76	1.96
V.E #17	V(kV)	1.00	1.96	3.00	4.00	5.02	6.00	6.96	8.00
	I(mA)	0.280	0.576	0.880	1.14	1.44	1.68	2.04	6.08

According to the data in Table 2.1, MOSA valve elements #5, #12 and #17 are very aged or damaged, #4, #6 and #7 may be aged, and the others are unaged. These valve elements have also been used in previous work [7, 12]. The classification of the elements is the same as before. The v-i_r characteristics of all these valve elements were obtained by using the compensation technique to classify the MOSA valve elements exactly.

2.1.2 Compensation Technique [7]

As mentioned in Chapter 1, a metal oxide valve element can be modeled as a non-linear resistor in parallel with a capacitor. Fig. 2.2 shows the simplified model considered in this thesis.

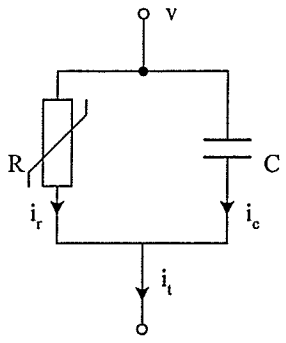

Fig. 2.2 Simplified model of MOSA valve element

If the applied voltage is pure sinusoidal, i.e., $v = v_1$, then $i_c = i_{c1}$. If a suitable G is selected to satisfy

$$i_r = i_t - G v_{s0} \tag{2-1}$$

where v_{s0} is the voltage v phase shifted forward by 90°, G is a constant which

corresponds to ωC where C is the capacitance in Fig. 2.2.

$$G = \omega C \tag{2-2}$$

Then

$$\int_0^{2\pi} v_{s0}(i_t - G v_{s0}) d(\omega t) = 0 \tag{2-3}$$

Eq.2-3 can be taken as the criteria for the complete compensation of the capacitive component in an R-C circuit, and the resistive component i_r can be calculated from Eq.2-1.

Unfortunately, the system voltage is seldom a pure sinusoid and consists of harmonic components. We can represent voltage as

$$v = \sum_n v_n \tag{2-4}$$

In this case the integral in Eq.2-3 does not vanish. Therefore, the criteria in Eq. 2-3 should be modified as

$$\int_0^{2\pi} v_{1s0}(i_t - G v_{1s0}) d(\omega t) = 0 \tag{2-5}$$

In the above equation, v_{1s0} is the fundamental component of v_{s0} and G has the same significance as explained above. Once the value of G is obtained, the equivalent capacitance C can be computed according to Eq. 2-2.

Applying FFT to the discrete voltage signals, the magnitude and phase angle of the fundamental voltage component v_1 can be found. Using the modified criteria of Eq. 2-5, the value of G may be obtained. As shown in Fig. 2.3, G is equal to 2.208×10^{-7}, therefore the value of equivalent capacitance C of an unaged MOSA valve element #9 is 584.19pF.

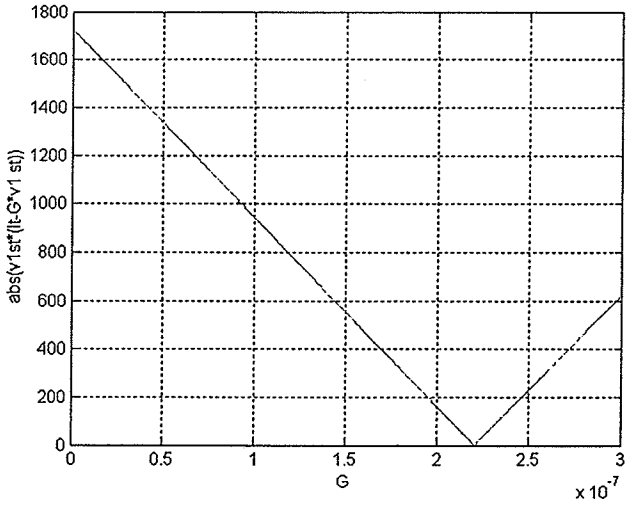

Fig. 2.3 Calculation of the equivalent capacitance of MOSA valve element #9

The equivalent capacitance value of all the MOSA valve elements used in the experiments were obtained in a similar manner.

2.1.3 v-i_r Characteristics of MOSA Valve Element

Having obtained the fundamental and harmonic components of the applied voltage and the capacitance value, it is easy to calculate the capacitive current due to the fundamental voltage and other harmonics present in the applied voltage.

The corresponding capacitive current can be written as

$$i_c = \sum_n n\omega C v_{n0}, n = 1,2,3,... \qquad (2\text{-}6)$$

where v_{n0} is the n^{th} order harmonic voltage phase shifted forward by 90°.

Since the voltage magnitudes of the harmonics above the 11^{th} order are usually small, the capacitive component due to these voltages may be neglected. Finally, we can

compute the resistive current by removing the capacitive component from the total current as in Eq. 2-7.

$$i_r = i_t - \sum_n n\omega C v_{n0}, n = 1,2,3,...,11 \qquad (2\text{-}7)$$

The corresponding v-i_r curve for valve element #9 is shown in Fig. 2.4.

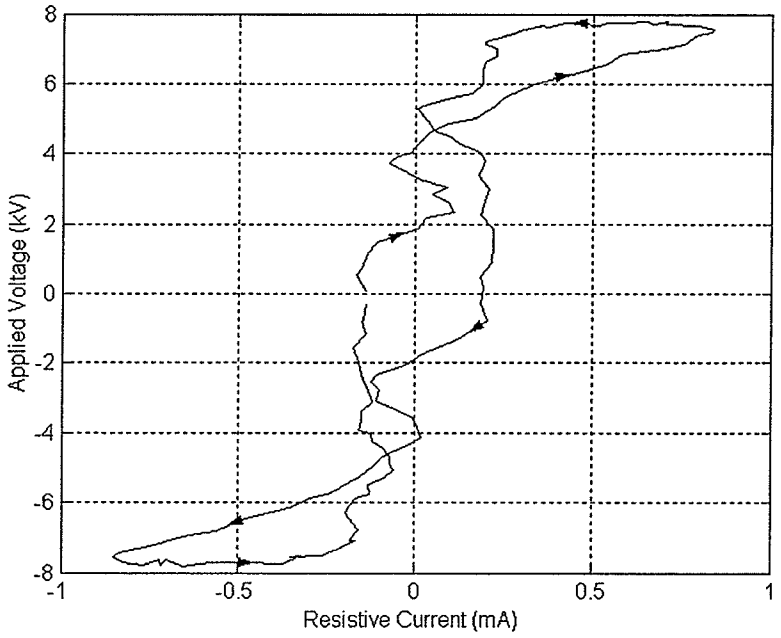

Fig. 2.4 v-i_r characteristic of MOSA valve element #9
(voltage and current are given as peak values)

The v-i_r characteristic in Fig. 2.4 shows a hysteretic behavior. An explanation of this behavior is beyond the scope of this thesis.

Similarly, the v-i_r characteristics of the same valve element at different test voltages can be obtained.

2.1.4 Derivation of Simplified v-i_r Characteristics

2.1.4.1 Simplified v-i_r Characteristics

From the above details, we know that use of the hysteretic v-i_r characteristics of a MOSA valve element in simulation studies is not practical since it requires determination of the characteristics at many voltages covering the expected range of voltage variations in the simulation. In this work, simplified v-i_r characteristics have been used. The simplified v-i_r characteristic is the locus of the tips of the hysteretic v-i_r characteristic obtained at different test voltages. Fig. 2.5 shows the simplified v-i_r characteristic of MOSA valve element #9.

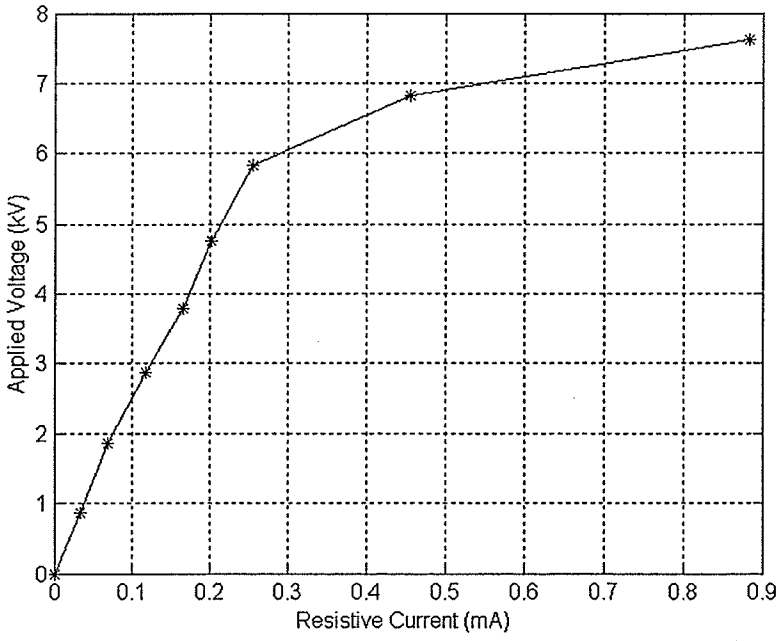

Fig. 2.5 Simplified v-i_r characteristic curve of MOSA valve element #9
(voltage and current are given as peak values)

The simplified v-i_r characteristics of other MOSA valve elements were obtained

using the same method described above. Some typical v-i_r characteristic curves are displayed in Fig. 2.6. In figures 2.5 and 2.6 the experimental points have been joined together with straight line segments.

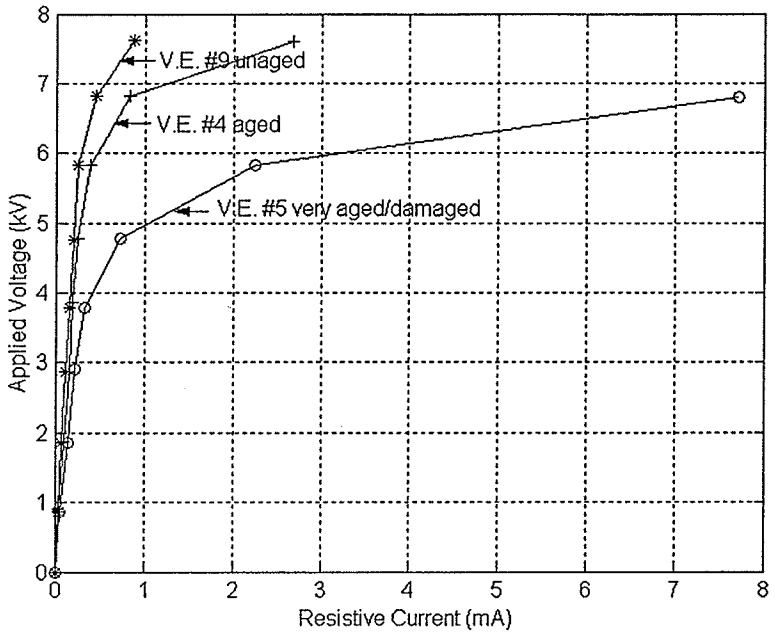

Fig. 2.6 Typical simplified v-i_r characteristic curves of aged, damaged/very aged and unaged MOSA valve elements (voltage and current are given as peak values)

2.1.4.2 Polynomial Representation of Simplified v-i_r Characteristics

In order to simulate the MOSA behavior in the low electric field region, a multi-segment polynomial representation is proposed because an exponential representation results in serious error [7]. From examination of the data in Fig. 2.5, it is obvious that the v-i_r characteristic is prominently nonlinear for $v > 0.8$ p.u.. For $v \leq 0.8$ p.u. the nonlinearity, although evident, is not as pronounced. Therefore, a two

segment polynomial representation is proposed. It was found that a good fit could be achieved by using a fifth order polynomial representation. In the voltage range $v \leq 0.8$ p.u., the polynomial representation for valve element #9 is given by:

$$i_r = 8.1423v^5 - 15.2239v^4 + 9.7982v^3 - 2.3201v^2 + 0.4152v \quad (2\text{-}8)$$

and for the voltage greater than 0.8 p.u., the representation is:

$$i_r = (0.3717v^5 - 1.6451v^4 + 2.9086v^3 - 2.5680v^2 + 1.1322v - 0.1994) \times 10^5 \quad (2\text{-}9)$$

The polynomial representation and the experimental data are both shown in Fig. 2.7 for comparison purposes. In Fig. 2.7, the stars signify the experimental data and the solid line represents the polynomial representation. It can be seen that the polynomial representation achieves an accurate fit. Simplified v-i_r characteristic for aged and damaged elements were also obtained and handled in a similar manner.

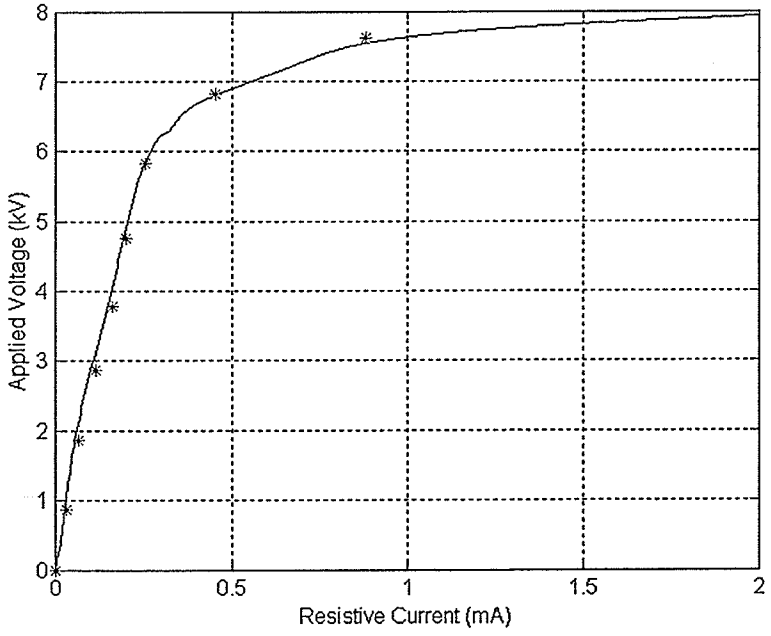

Fig. 2.7 Polynomial representation of experimental v-i_r characteristic (voltage and current are given as peak values)

Using the polynomial expression Eq.2-9 valid for unaged valve element #9 the voltage necessary to cause 1 mA of peak resistive current is found to be 0.9832 p.u.. Using expressions similar to Eq.2-9 but for aged (V.E #4) and damaged elements (V.E #5) the voltages necessary to cause 1 mA of peak resistive current are 0.8888 p.u. and 0.6198 p.u. respectively, which are 9.6% and 37.0% less than the corresponding voltage for an unaged element.

The polynomial equations can not be directly used in the simulation model discussed in Chapter 3. In the simulation model the nonlinear resistance is represented in the form of a data file that agrees with the v-i_r characteristic. This will be described in Chapter 3.

2.2 Neutral Current Method

Having found the voltage-current characteristics of MOSA valve elements, they were used to examine the suitability of the neutral current method for on-site diagnostic testing for MOSA. The neutral current method was applied to combination of unaged, aged and very aged/damaged valve elements in the three phases using a three-phase laboratory setup.

2.2.1 Principle of the Neutral Current Method

As shown in Fig. 2.8, the neutral current, I_n, can be obtained from the neutral line using a shunt or a suitable current monitor. If metal oxide arresters in three phases are

identical and the applied three-phase voltage is purely sinusoidal and balanced, the sum of the three capacitive components of the arrester currents will be zero, and the neutral current I_n equals to $3I_{r3}$.

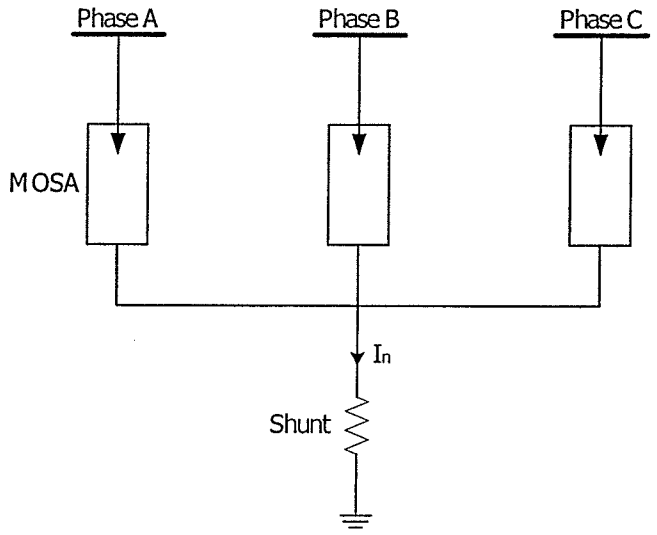

Fig. 2.8 Schematic diagram of the Neutral Current Method

If an arrester in one phase ages it will result in an increase in one of the peaks of the third harmonic wave shape in neutral current. This peak repeats every two cycles at third harmonic frequency. Therefore, it may be possible to use the neutral current as a diagnostic indicator to assess the MOSA condition in service. Identification of defective arrester is easy if phase voltage waveform is available.

2.2.2 Laboratory Setup for the Neutral Current Method

In order to investigate the neutral current method, a three-phase test circuit

(horizontal, flat configuration) shown in Fig. 2.9, was set up in the laboratory.

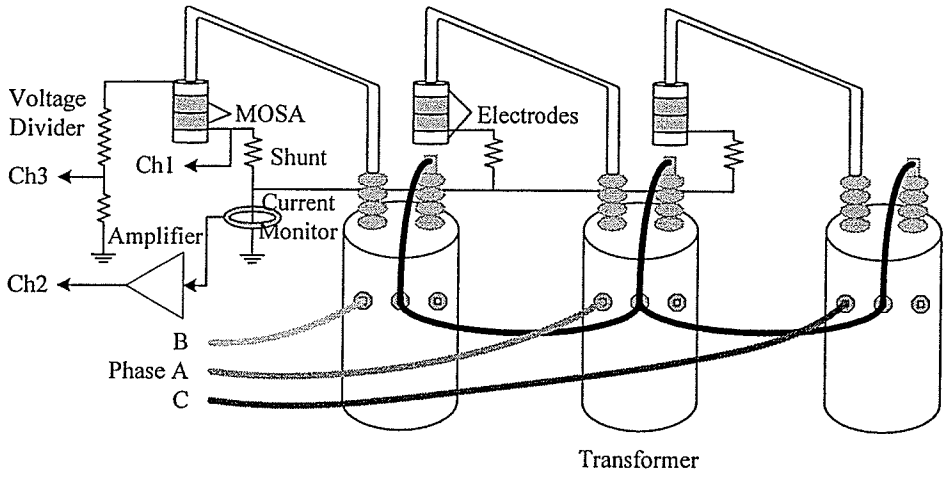

Fig. 2.9 Laboratory setup for three-phase arrester configuration, MOSA comprised of two valve elements in each phase

In Fig. 2.9, the three 120/14400 V, 10 kVA distribution transformers are Y/Y connected. The MOSA in each phase is comprised two valve elements. The bottom edge of each MOSA column is grounded through a 10 kΩ resistive shunt. Insertion of a current monitor in the neutral ground wire allows the neutral current to be detected. The current monitor used was Pearson Electronics Standard Current Monitor, model 411, with a sensitivity of 0.1volts/amp. It was found that the monitor was not sensitive enough. In order to increase its sensitivity, 20 turns of the current lead were looped through the opening of the current monitor. In addition, the output of the current monitor was fed to an amplifier which amplified the detected signal to be displayed by the oscilloscope. A high voltage probe, the resistive divider, which has a ratio of 1000:1 (100 MΩ/10 kΩ) in

Fig. 2.9, was used to measure the applied phase voltage. A four-channel digital storage oscilloscope TEK TDS 3054 was used to capture and display all these signals simultaneously.

In order to check the accuracy of the current monitor-amplifier combination a voltage equal to the chosen MCOV value was applied to the three-phase configuration with two unaged valve elements per phase. The neutral current measured by using the current monitor was compared with that measured by use of a resistive shunt. In addition, all three phase currents were measured to check if their sum equals the measured value in the neutral lead. The peak values of the neutral current measured by resistive shunt, current monitor and the sum of three phase currents are shown in Table 2.2.

Table 2.2 Peak values of the neutral current

Peak Value (mA)	Sum of three phase currents	Resistive shunt	Current monitor
Positive cycle	0.8415	0.8205	0.8000
Negative cycle	0.9230	0.9026	0.9400

From Table 2.2 it is seen that the current monitor system can measure the neutral current with an error less than 0.05 mA.

2.2.3 Application of the Neutral Current Method

By using the three-phase configuration in Fig. 2.9, a voltage (11 kV, LN RMS) was applied to MOSA comprised of two valve elements per phase and waveforms of the total

current in each phase (using resistive shunts) and the neutral current (using the current monitor) plus the waveform of one phase voltage were recorded for the following cases.

2.2.3.1 Unaged MOSA in All Three Phases

Unaged MOSA valve elements (#2 & #9 in phase C, #10 & #11 in phase A, #14& #16 in phase B) were used in the three-phase configuration. Fig. 2.10 shows waveforms of the total current per phase and the phase A voltage. Fig. 2.11 shows waveforms of the total current in phase A, neutral current and the phase A voltage.

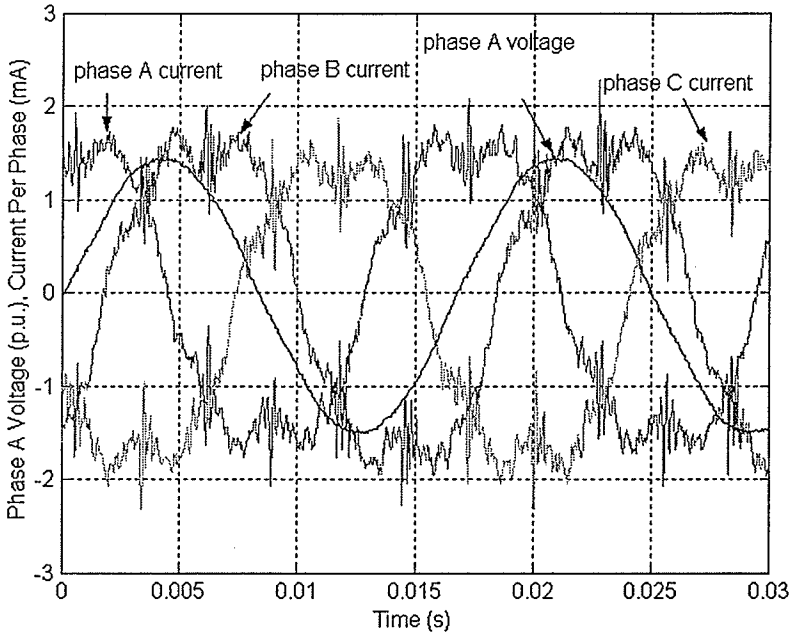

Fig. 2.10 Total current in each phase and phase A voltage waveforms. Unaged MOSA valve elements in each phase

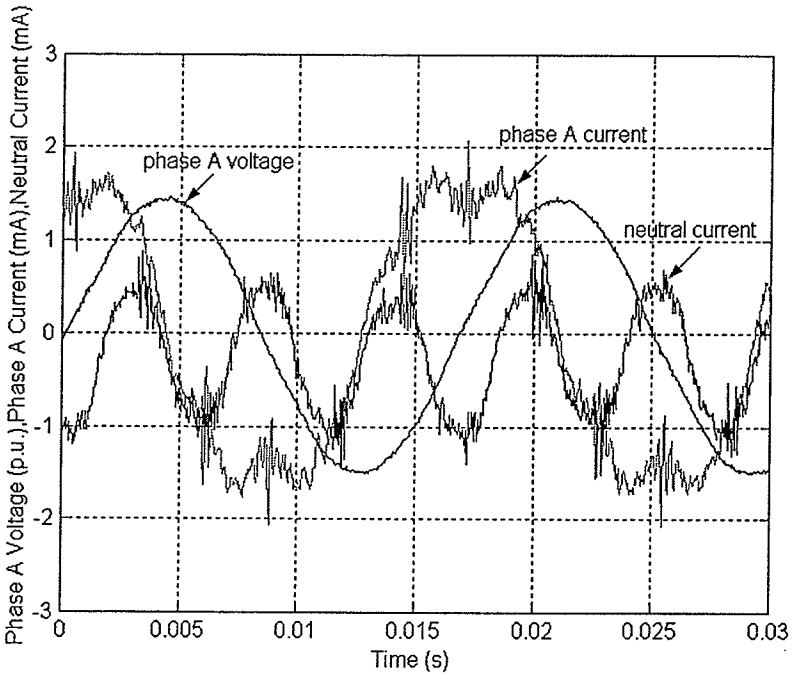

Fig. 2.11 Phase A voltage, total current and neutral current waveforms. Unaged MOSA valve elements in each phase

From Fig. 2.11 it can be seen that the neutral current is of a rather uniform third harmonic. The current waveforms are not symmetrical about the zero line because the valve elements are not new and their characteristics are not identical. Comparing the waveforms of the total current in phase A and the phase A voltage waveform, we can see that the peak of the current waveform is almost 90° ahead of that of the voltage waveform. This is due to the dominance of the capacitive component for unaged MOSA valve elements under rated voltage.

2.2.3.2 Aged MOSA in Only One Phase

Case 1: One aged MOSA valve element in phase C

One aged MOSA valve element was used instead of an unaged valve element in phase C of the three-phase configuration in section 2.2.3.1: #4 & #9 in phase C, #10 & #11 in phase A, #14 & #16 in phase B.

Fig. 2.12 shows waveforms of the total current in each phase and the phase A voltage. In Fig. 2.12, the total current in phase C has a higher peak value when compared with the other two phase currents. Theoretically, this higher current due to the defective MOSA valve element in phase C should result in an increase in one of the peaks of the third harmonic wave shape in neutral current.

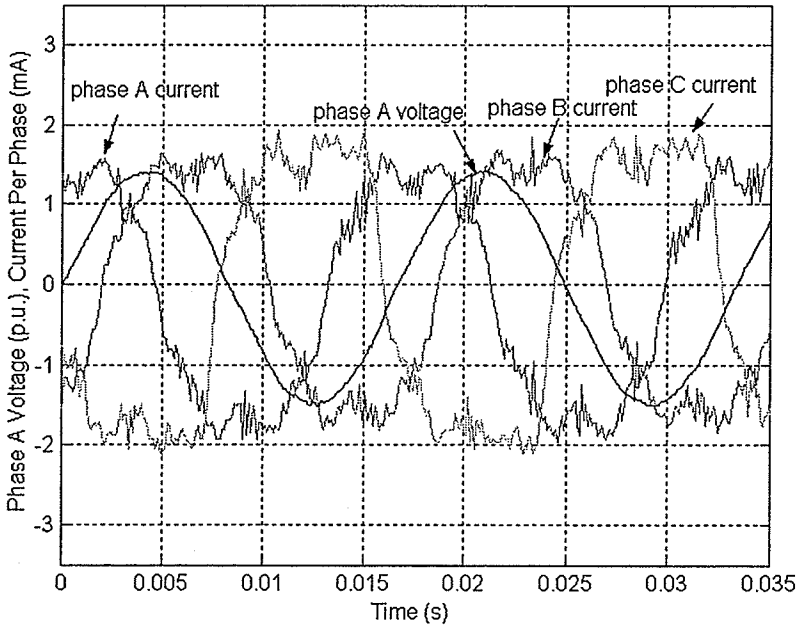

Fig. 2.12 Total current in each phase and phase A voltage waveforms for case 1

The waveforms of the total current in phase A, neutral current and the phase A voltage are shown in Fig. 2.13.

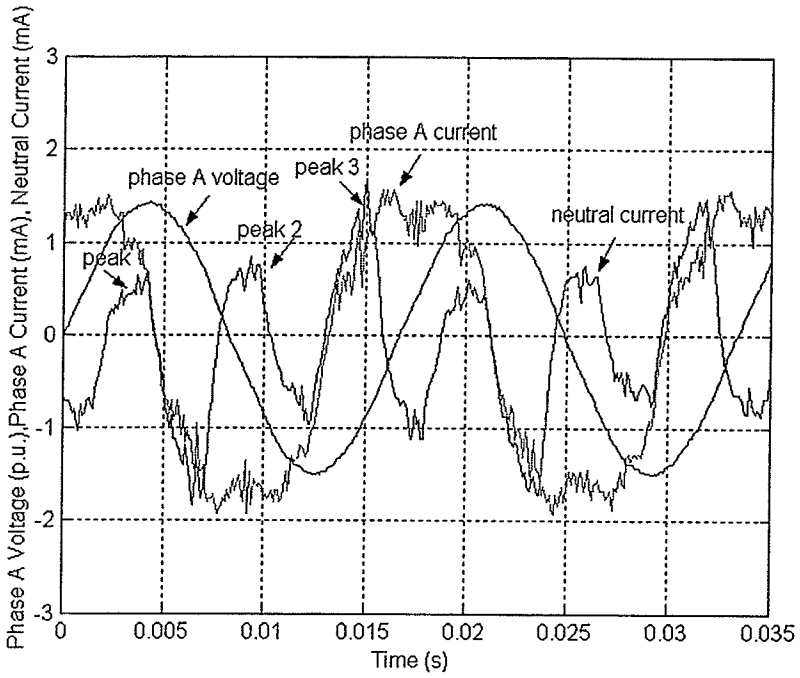

Fig. 2.13 Phase A voltage, total current and neutral current waveforms for case 1

In fact, from the experimental results shown in Fig 2.13, there is an increase in the peak of the third harmonic wave shape in neutral current and this peak repeats every two cycles at third harmonic frequency. The three peaks of the neutral current, peaks 1, 2, and 3 within one cycle of the phase A voltage, corresponds to phases A, B and C respectively. The peaks of the resistive neutral current almost coincide with the peaks of the voltage in each phase. The largest peak in the neutral current is almost 240° removed from the peak of the phase A voltage. Since the phase sequence is ABC, it can be inferred that the defective valve element is situated in phase C.

Case 2: Two aged MOSA valve elements in phase C

Both MOSA valve elements in phase C were of the aged type while the valve elements in other two phases were unaged: #4 & #6 in phase C, #10 & #11 in phase A, #14 & #16 in phase B. The waveforms of the total current in each phase and the phase A voltage are shown in Fig. 2.14.

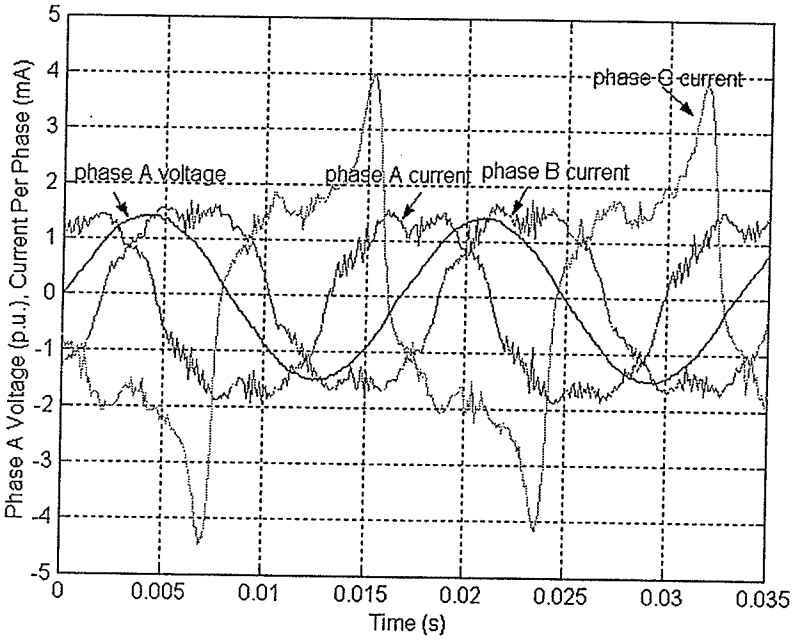

Fig. 2.14 Total current in each phase and phase A voltage waveforms for case 2

From Fig. 2.14 it can be seen that the peak value of the total current in phase C is much higher than that of other two phases. This total current in phase C will register as an increase in the appropriate third half cycle in the neutral current. Fig. 2.15 shows waveforms of the total current in phase A, neutral current and the phase A voltage. It can be inferred that the defective MOSA valve elements are located in phase C when we refer

the neutral current waveform to the phase A voltage waveform.

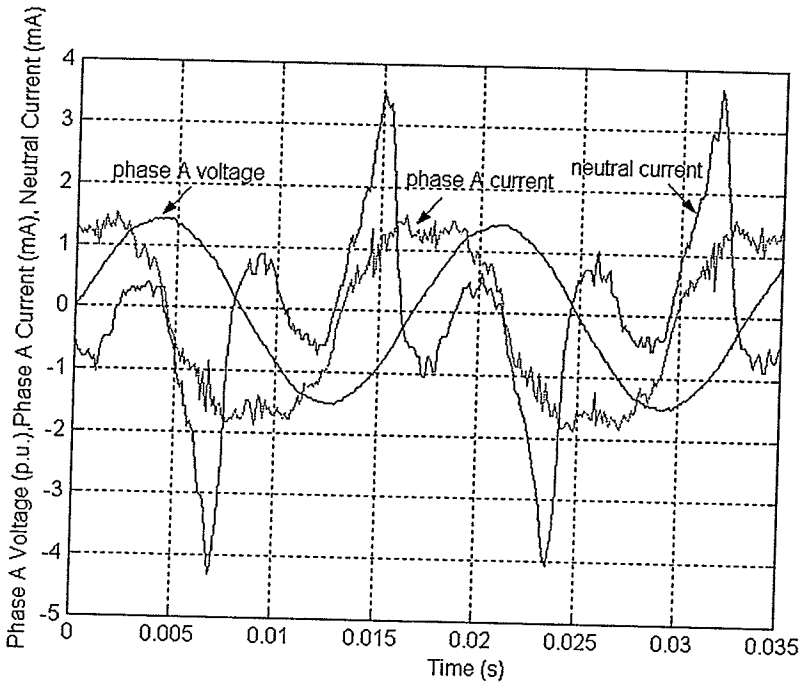

Fig. 2.15 Phase A voltage, total current and neutral current waveforms for case 2

Case 3: One damaged/very aged MOSA valve element in phase C

One damaged/very aged MOSA valve element is placed in phase C and the other valve elements are unaged in the three-phase configuration in Fig. 2. 9: #5 & #9 in phase C, #10 & #11 in phase A, #14 & #16 in phase B. Fig. 2.16 shows waveforms of the total current in each phase and the phase A voltage. Form Fig. 2.16, we can notice that the waveform of the total current in phase C is seriously distorted and has a high peak value due to the very aged MOSA valve element in this phase.

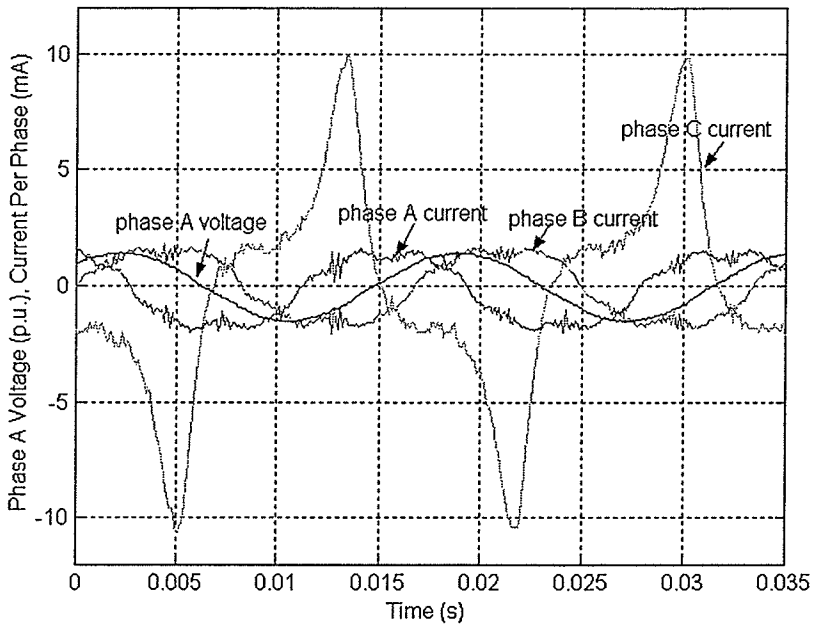

Fig. 2.16 Total current in each phase and phase A voltage waveforms for case 3

Fig. 2.17 shows waveforms of the total current in phase A, neutral current and the phase A voltage.

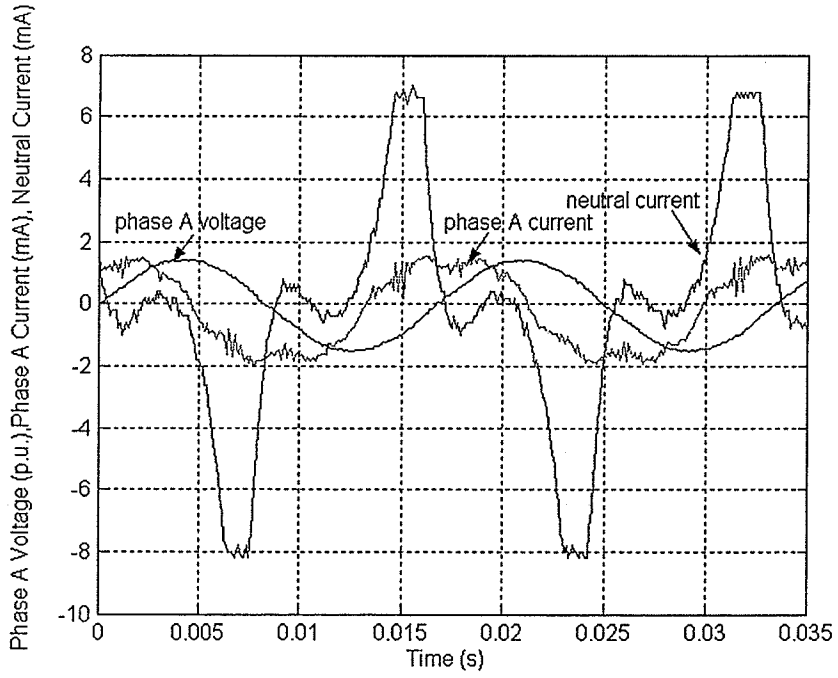

Fig. 2.17 Phase A voltage, total current and neutral current waveforms for case 3

As before, an increase in one of the peaks of the third harmonic wave shape in neutral current can be used to identify defective MOSA valve element in phase C by referring the three peaks in the neutral current waveform to the phase A voltage waveform.

Case 4: Two damaged/very aged MOSA valve elements in phase C

Two damaged/very aged MOSA valve elements were inserted in phase C: #5 & #12 in phase C, #10 & #11 in phase A, #14 & #16 in phase B. The waveforms of the total current in each phase and the phase A voltage are shown in Fig. 2.18.

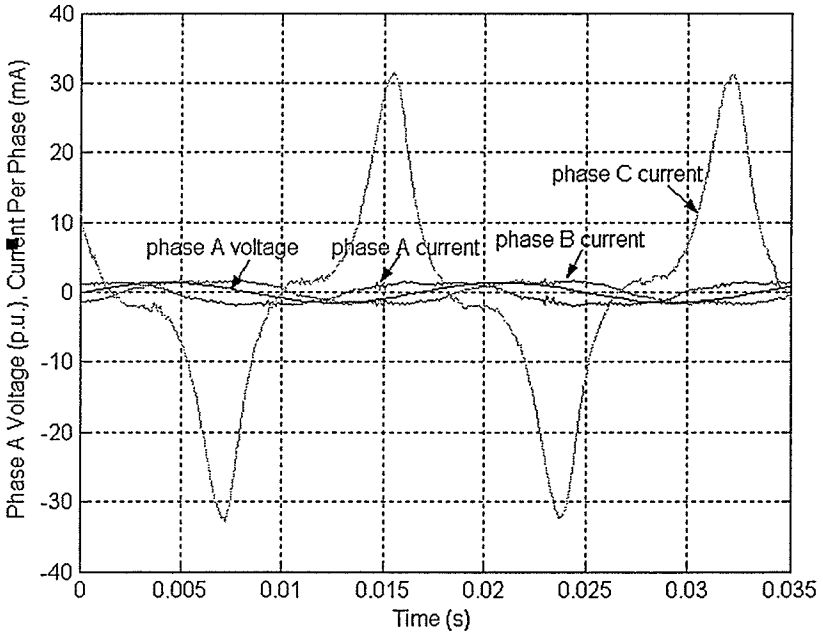

Fig. 2.18 Total current in each phase and phase A voltage waveforms for case 4

From Fig. 2.18 it can be seen that the peak value of the total current in phase C is

much higher than that of other two phases. If the phase A voltage is delayed by 240 degrees to obtain the waveform of the phase C voltage, it will be seen that the total current in phase C is almost in phase with the phase C voltage. This is because the resistive component in the total current of phase C is very large and dominates the total current due to the presence of the very aged valve elements. As a result, an extremely high peak in three peaks of the third harmonic wave shape will show up in the neutral current.

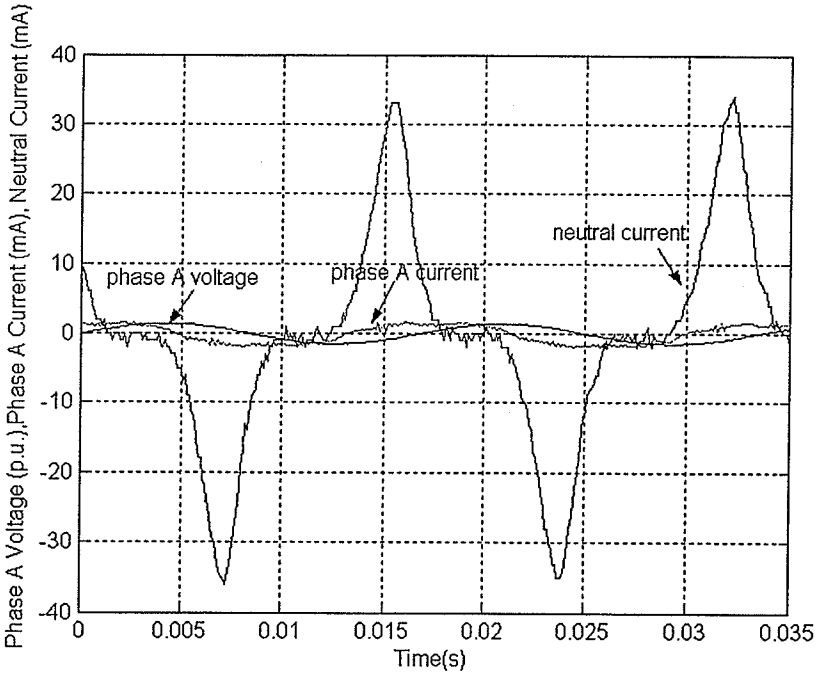

Fig. 2.19 Phase A voltage, total current and neutral current waveforms for case 4

Fig. 2.19 shows waveforms of the total current in phase A, neutral current and the phase A voltage. The neutral current waveform is seriously distorted compared with the neutral current of unaged valve elements in three-phase configuration as shown in Fig. 2.11. It can also be identified that this huge increase in one of the peaks in the neutral

current is the result of the defective MOSA valve elements present in phase C.

2.2.3.3 Aged MOSA in Two Phases

Case 5: One damaged/very aged MOSA valve element in phase A, and two aged valve elements in phase C

In this case, one damaged/very aged MOSA valve element was inserted in phase A, and two aged valve elements were used in phase C. The other two valve elements in phase B were unaged: #4 & #6 in phase C, #5 & #9 in phase A, #14 & #16 in phase B.

The waveforms of the total current in each phase and the phase A voltage are shown in Fig. 2.20.

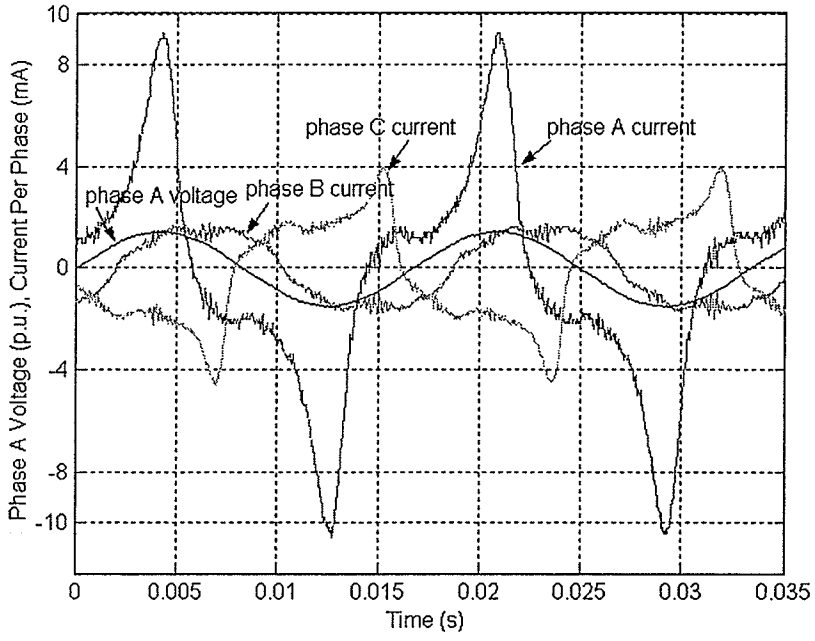

Fig. 2.20 Total current in each phase and phase A voltage waveforms for case 5

Fig. 2.21 shows waveforms of the total current in phase A, neutral current and the phase A voltage. From Fig. 2.21 one can identify that the MOSA valve elements in phase A and phase C are defective.

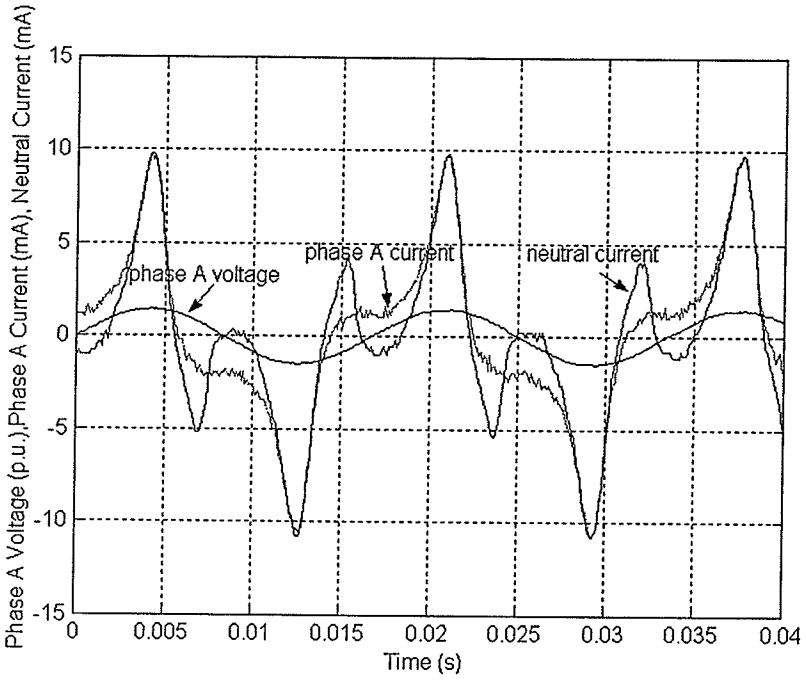

Fig. 2.21 Phase A voltage, total current and neutral current waveforms for case 5

2.2.4 Comments on Neutral Current Method

Experimental results show that the neutral current method can be used to assess the condition of the MOSA in a three-phase configuration if the applied phase voltage waveform is available simultaneously. Practically, it is not so easy to obtain the applied phase voltage waveform on-site which must be taken from a PT or a divider. Without a reference voltage, identification of the aged MOSA is not possible. In order to assess the

condition of MOSA in each of the three phases using the neutral current method, a slight modification of this method is necessary. This is discussed in the next section.

In addition, From Fig. 2.12 (all valve element in all three phases unaged), it is seen that the peak values of the neutral current are not equal because of the slightly non-identical v-i_r characteristics of MOSA. In practice, MOSA in the three phases are seldom identical, even if they are unaged. This may result in a misleading judgment. Therefore, for the successful implementation of this method the test results should be compared with test data on an ongoing basis.

2.3 LabVIEW Program for Phase Identification of the Aged Element or Elements

It is important for the neutral current method used as an on-site diagnostic technique to identify the defective phase and assess the condition of the MOSA in service. As mentioned above, a slight modification is necessary for the neutral current method to be used successfully as a diagnostic indicator. In this section, the modification is introduced. Furthermore, the required logic and computer program based on LabVIEW graphic language are developed for phase identification of the aged MOSA element or elements.

2.3.1 Use of the Neutral Current Method as a Diagnostic Indicator

A modification to the neutral current method is introduced to enable its application

on-site as a quick test to determine MOSA condition in a three-phase system.

Experimental results show that the peak of the total current in one phase of unaged MOSA sets operated at its MCOV is approximately 90° ahead of the peak of the corresponding applied phase voltage because the capacitive current dominates in the low electric field region. Therefore, a phase current waveform can be recorded and shifted to obtain a reference waveform with almost the same phase as the applied phase voltage so that the problem of acquisition of the applied phase voltage can be overcome.

Using suitable current monitors simultaneously in one phase and the neutral enables the identification of an aged MOSA during on-site diagnostic test. A test circuit for accomplishing this is shown in Fig. 2.22. Current monitor CM_1 may be inserted in any phase while current monitor CM_2 is inserted in the common neutral line.

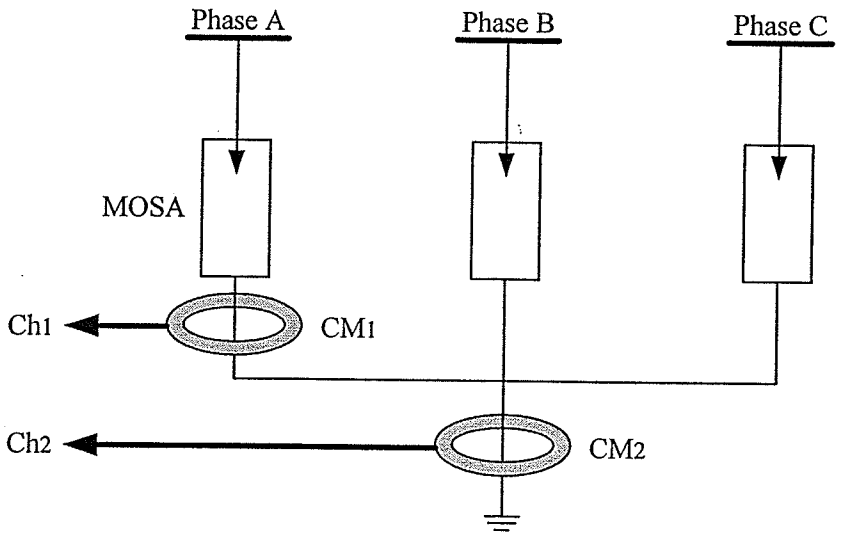

Fig. 2.22 Measurement setup for use of the neutral current method as a diagnostic indicator

The two signals from CM_1 and CM_2 are amplified and sampled through the sampling unit. The sampled signals are input into a microprocessor. In the microprocessor, the phase current in phase A and neutral current waveshapes can be analyzed.

2.3.2 Principle of Computer Program

Once the amplified phase current and the neutral current signals are obtained, analysis is processed by computer program to give the identification results. In this process, a low pass filter is used to remove the high frequency noise in the two current signals. A phase current waveform is delayed by 90° to obtain a reference waveform.

Next, the three peak values I_1, I_2, I_3 of the neutral current and the corresponding times t_1, t_2, t_3 of occurrence of these peaks are identified within one cycle of the reference waveform (0.01667sec) starting from its positive-going zero. Comparing these time values with the time corresponding to the peak value of the shifted phase current, the three peaks can be related to three phases. The neutral current peak closest to the zero of the reference waveform is identified as belonging to the phase number which is the same as that used to obtain the reference waveform. The RMS value of the neutral current, I_0, can also be easily calculated. The minimum of the three peaks in the neutral current is marked as I_{min}, which is used as a reference for three-phase identification. Next, the waveshape factors, $k_{1(2,3)}=I_{1(2,3)}/I_{min}$, are calculated and displayed. Comparing these three waveshape factors with experience-derived criteria, the MOSA condition in the three

phases can be obtained and displayed. When k_x (x=1, 2 or 3) is abnormal, a message may be displayed instructing the operator to change the MOSA in service. The flow chart of the computer program used for phase identification is shown in Fig. 2.23.

Here, the criteria are deduced from laboratory experimental data. From the experimental runs the neutral current peaks were measured for various cases discussed in section 2.2.3. From the data and [13] the following criteria is suggested.

$k_x \leq 2$, phase x is unaged;

$2 < k_x < 5$, phase x is aged;

$k_x \geq 5$, phase x is damaged

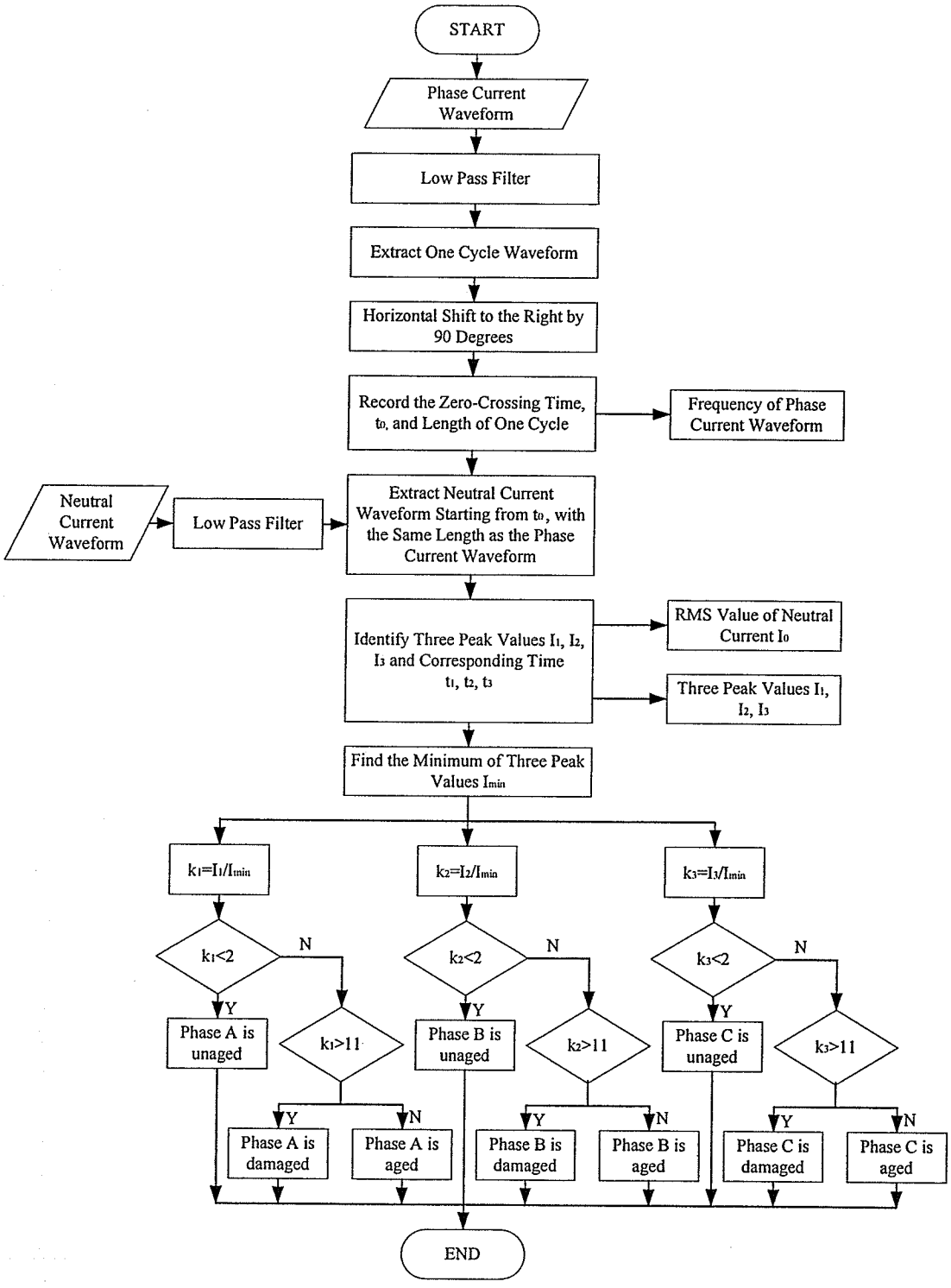

Fig. 2.23 Flow chart of the computer program used for phase identification of aged valve element

2.3.3 LabVIEW Program Used for Identification

LabVIEW is a universally used software nowadays. Using LabVIEW virtual instruments to perform analysis operations makes the display of identification results easily visible. In addition, LabVIEW can be installed in any laptop computer thus ensuring portability of the diagnostic technique.

Data acquisition board AT-MIO-16E-2 from National Instruments together with 5B41 voltage input module (signal conditioner) was used to acquire the signals. The LabVIEW virtual instrument panel is shown in Fig. 2.24.

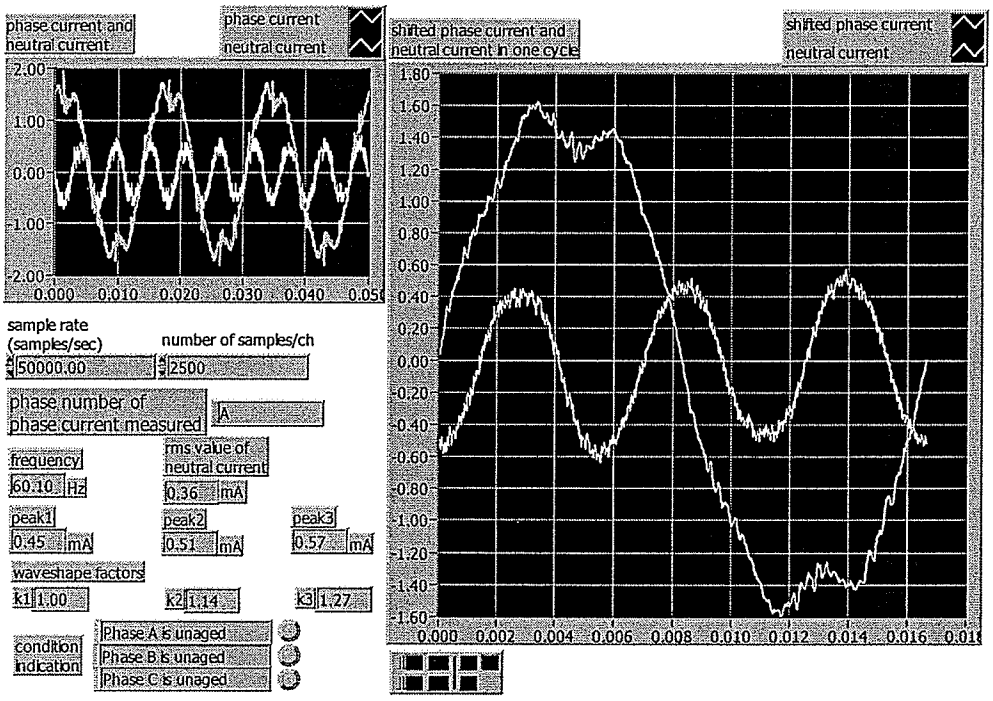

Fig. 2.24 Display of the LabVIEW virtual instrument panel for unaged case

There are two main sections in the panel. One is control input section, and the other

is the indicator section. The sample rate and number of samples per channel are dependent on the data acquisition board and input manually. The phase number of the phase current, which is measured along with the neutral current, is also input by the operator. The indicator section includes: frequency of the phase current, rms value of the neutral current, the three peak values of the neutral current, three waveshape factors, phase current and neutral current waveforms, and one waveform window to display the shifted phase current and the neutral current waveform for a duration of one cycle. The condition of the MOSA in all three phases is also displayed. If there is a defective phase, the LED alarm will light and ring.

In order to assess the condition of MOSA the operator needs to measure the neutral current and a current in one chosen phase. Three cases arise.

Case a: The phase chosen to measure the phase current contains unaged MOSA.

Case b: The phase chosen to measure the phase current contains an aged MOSA.

Case c: The phase chosen to measure the phase current contains a damaged MOSA.

The LabVIEW waveforms of virtual instrument panel readouts corresponding to each of the above cases is shown below.

Case a: The chosen phase contains unaged MOSA

In this case the defective MOSA, an aged MOSA (V.E #4) was in phase C and the MOSA in the remaining phases were unaged: #4 & #9 in phase C, #10 & #11 in phase A, #14 & #16 in phase B. The operator chooses to measure the phase A current to obtain the

reference waveform. Fig. 2.25 shows the display obtained. The program logic correctly identifies the aged MOSA to be in phase C.

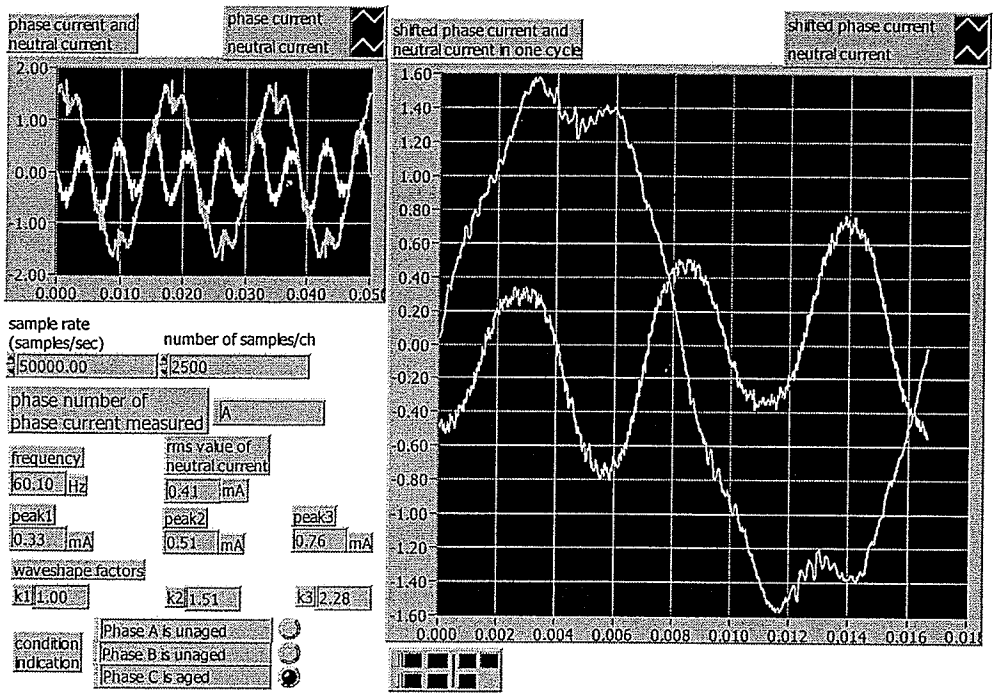

Fig. 2.25 Display of the LabVIEW virtual instrument panel for case a with an aged valve element in phase C

Fig. 2.26 shows display of the LabVIEW virtual instrument panel obtained when the defective MOSA (V.E #5) in phase C is damaged. Once again, the reference waveform was obtained from the phase A current. Fig. 2.26 shows that the program logic correctly identifies the damaged MOSA to be in phase C.

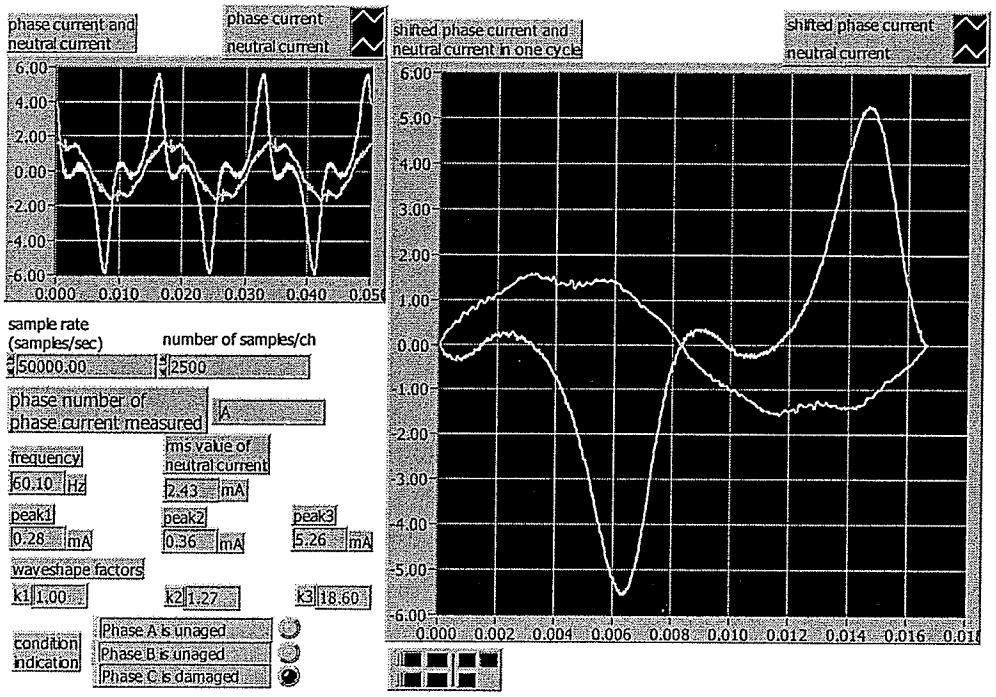

Fig. 2.26 Display of the LabVIEW virtual instrument panel for case a with a damaged valve element in phase C

Case b: The chosen phase contains an aged MOSA.

In this case the defective MOSA, an aged MOSA, was in phase C. The MOSA in the remaining two phases were unaged: #4 & #9 in phase C, #10 & #11 in phase A, #14 & #16 in phase B. The operator chooses to measure the phase C current to obtain the reference waveform. Fig. 2.27 shows the display obtained. The program logic correctly identifies the aged MOSA to be in phase C.

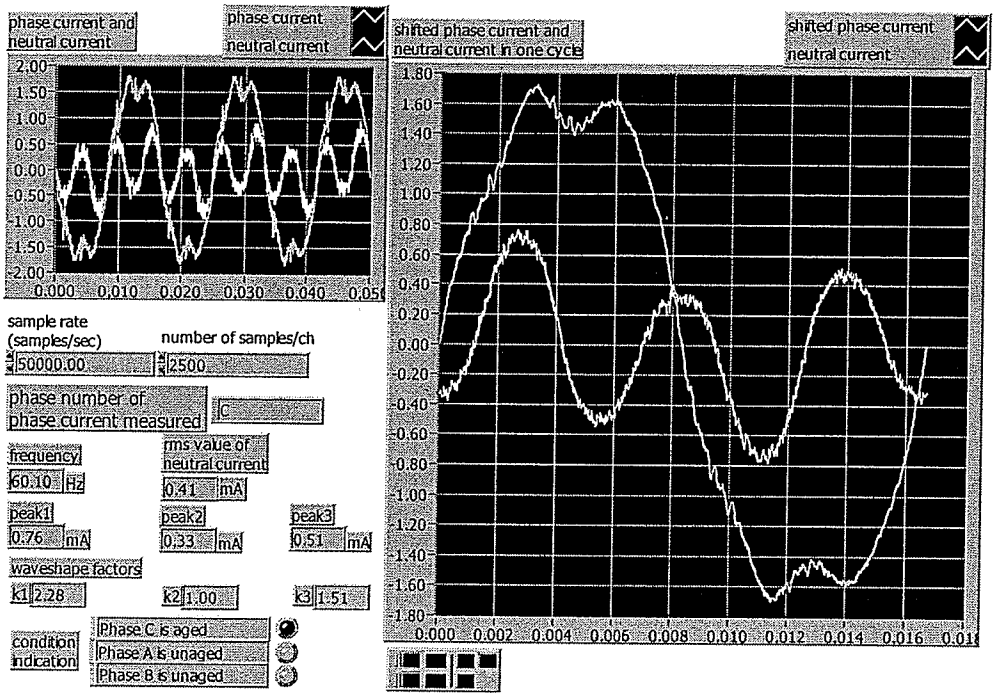

Fig. 2.27 Display of the LabVIEW virtual instrument panel for case b

Case c: The chosen phase contains a damaged MOSA.

In this case the defective MOSA, a damaged MOSA (V.E #5), was in phase C. The MOSA in the remaining two phases were unaged: #5 & #9 in phase C, #10 & #11 in phase A, #14 & #16 in phase B. The operator chooses to measure the phase C current to obtain the reference waveform. Fig. 2.28 shows the display obtained. The program logic correctly identifies the damaged MOSA to be in phase C.

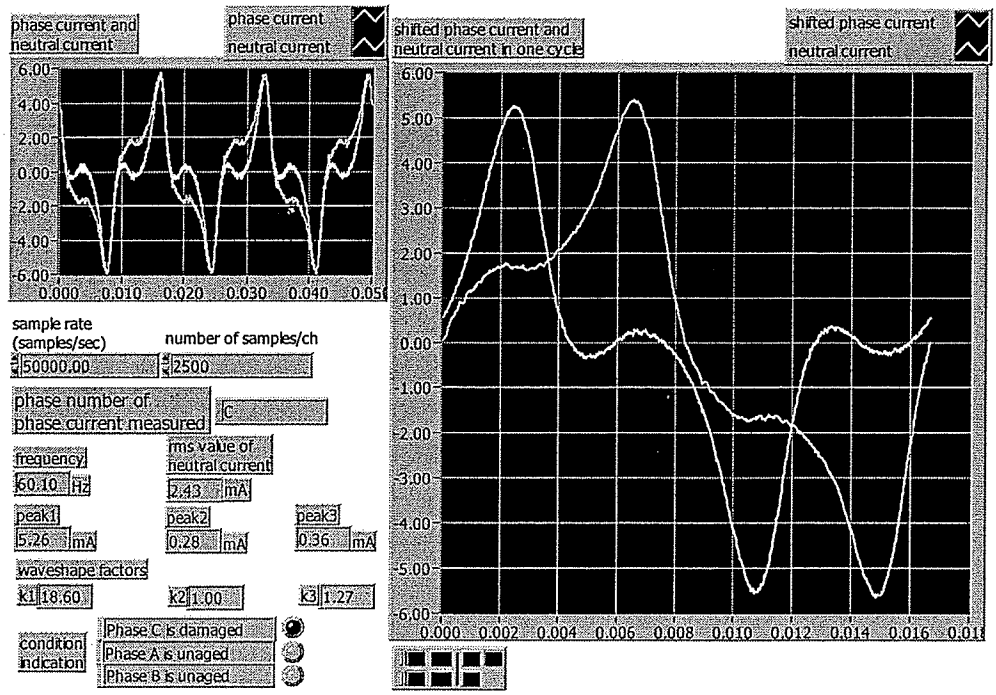

Fig. 2.28 Display of the LabVIEW virtual instrument panel for case c

The above shows that the LabVIEW virtual instrument programmed with logic as outlined in section 2.3.2 is able to satisfactorily diagnose the condition of MOSA in a three phase setup in a laboratory setting.

The suggested neutral current diagnostic method identifies the three successive peaks of the neutral current and computes the ratio k. Since $k_{1(2,3)}=I_{1(2,3)}/I_{min}$ and $I_{min}= I_1$ or I_2 or I_3, one of the k will be always equal to unity. Assessment of the MOSA condition is based on the remaining k values. The method will therefore work satisfactorily if at least one of the MOSA is unaged. To enable the method to function satisfactorily when this condition is not met, a modification is necessary in the program logic which may be

implemented using one of two approaches outlined below.

Approach A: In this method the neutral current diagnostic method is applied immediately after installation of new arresters whose condition has been verified in a laboratory setting. The three peaks of the neutral current are obtained and the smallest peak classified as a benchmark value (I_{BM}). In subsequent measurements if none of the ratios of the neutral current peaks to the benchmark value i.e. I_n (n=1, 2, 3)/ I_{BM} is less than 2, this means that none of the phases contains unaged MOSA and the program will directly indicate that all three phases are defective. If at least one of the ratios is less than 2, the program will execute as before mentioned as in section 2.3.2 and fulfill the phase identification.

Approach B: The neutral current peaks are almost equal to the peak value of the resistive current in the corresponding phase as the following experimentally derived data in Table 2.3 shows.

Table 2.3 Neutral current peak value and resistive current of the corresponding phase

Condition of MOSA Valve Elements in Phase			Neutral Current Peak Corresponding to Phase A (mA)	Peak Values of Resistive Current of Valve Elements in Phase A (mA)
A	B	C		
Unaged V.E #10& #11	Unaged V.E #14& #16	Unaged V.E #2& #9	0.80	0.7983
Damaged V.E #5& #9	Unaged V.E #14& #16	Aged V.E #4& #6	9.80	9.7796

Therefore one may assign a benchmark value based on laboratory tests from which the resistive current values of unaged arresters are obtained. The logic then proceeds as in approach A. Fig. 2.29 shows the modified flow chart of the computer program to take into account the possibility that none of the phases contains unaged MOSA.

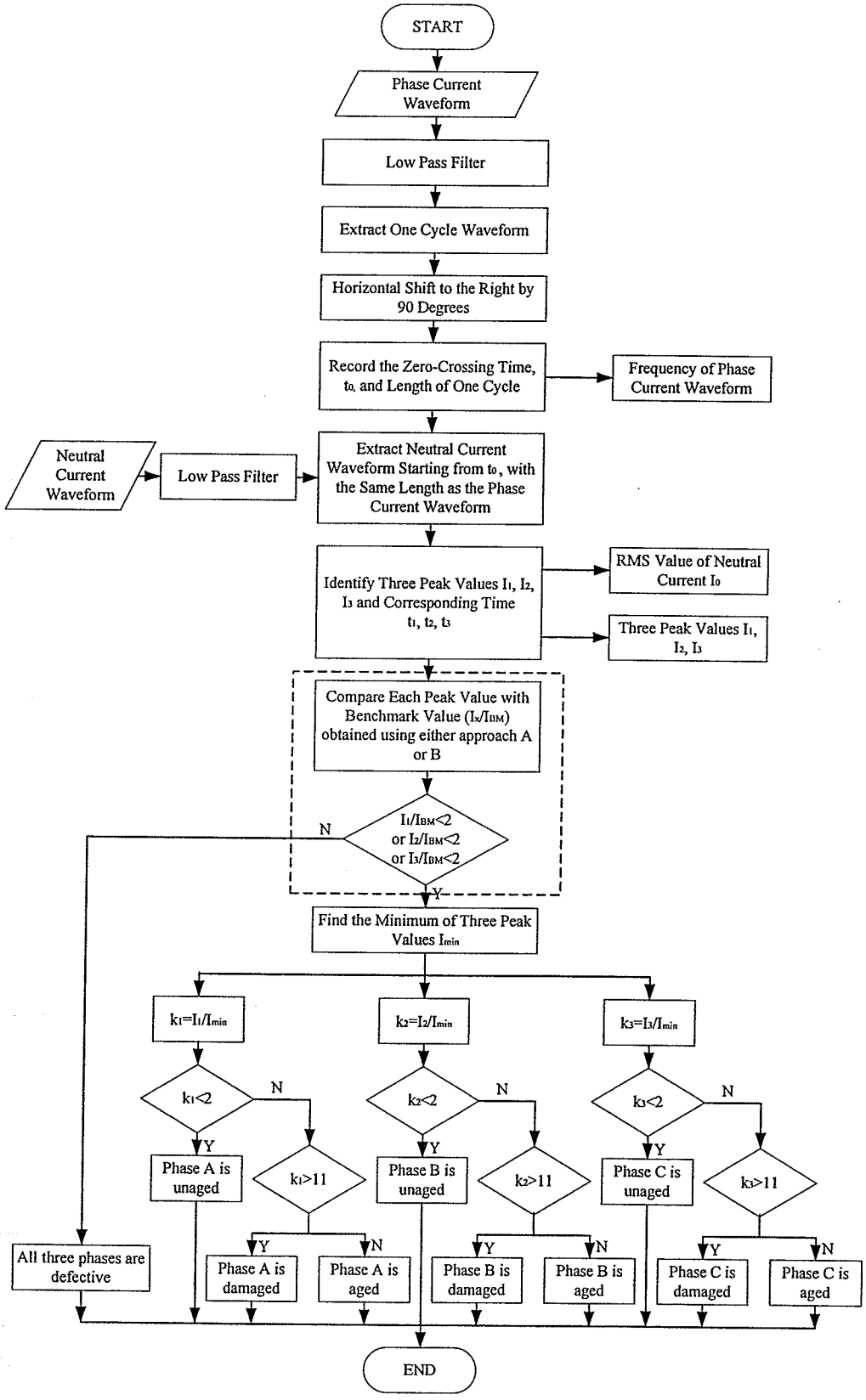

Fig. 2.29 Required Modification to flow chart of the computer program

CHAPTER 3

Influence of Inter-phase Interference, Harmonic Voltages and Unbalanced Phase Voltage on the Neutral Current Method Used as a Diagnostic Indicator

In this chapter, the influences of inter-phase interference, harmonics in the supply voltage and unbalanced phase voltage on the neutral current method used as a diagnostic indicator are examined. The influence of inter-phase interference on the neutral current as a diagnostic indicator of MOSA in service is experimentally investigated. The errors introduced due to the presence of harmonics in system voltage and unbalanced phase voltage are investigated by using PSCAD/EMTDC^{+}.

3.1 Influence of Inter-phase Interference on the Neutral Current Method

The stray capacitance between neighboring phases may result in errors in the resistive current per phase obtained by implementation of the compensation method [7]. However, the influence of stray capacitance between neighboring phases may not be reflected in the neutral current.

Fig. 3.1 shows the three-phase diagram with stray capacitances C_{ab} and C_{ac}. Because

of the presence of stray capacitances, the current in the three phases may not be identical (even with identical valve elements). However since the stray capacitance magnitude is small their influence may be negligible and therefore one may expect that the inter-phase interference has little or no influence on diagnostics based on the neutral current method.

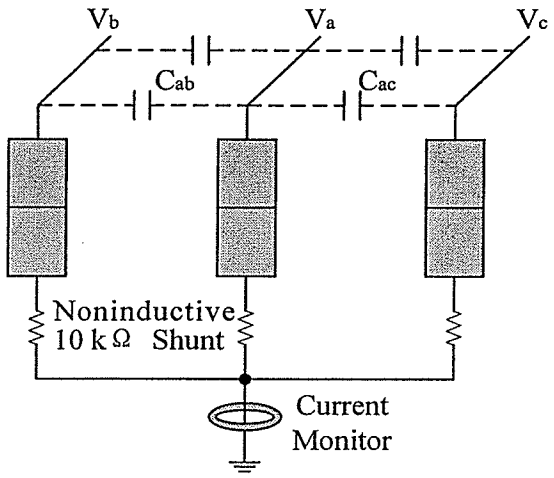

Fig. 3.1 Three-phase diagram with influence of the neighboring phases

In the laboratory setup the distance between two adjacent phases was halved in order to examine the influence of inter-phase interference. The neutral current waveform recorded with the two configurations was compared with unaged elements in all three phases and with one aged element in phase C (outer phase). It was found that the neutral current waveforms obtained with the two configurations (original inter-phase clearance and halved inter-phase clearance) overlap. Table3.1 shows a comparison of the three peak values of the neutral current. Here, Peaks 1, 2, 3 correspond to phases A, B and C respectively.

Table 3.1 Three peak values of the neutral current obtained from different phase-distance configurations

Case	Distance Between Adjacent Phases		Peak Value of the Neutral Current (mA)		
	(inch)	(cm)	Peak1	Peak2	Peak3
Unaged Elements in Three Phases	32	81.28	0.48	0.52	0.55
	16	40.64	0.49	0.54	0.62
One Aged Element in Phase C	32	81.28	0.33	0.51	0.76
	16	40.64	0.37	0.51	0.76

These results show that the three peak values of the neutral current change only slightly when the distance between adjacent phases is decreased to half. It demonstrates that the inter-phase interference has a negligible influence on the neutral current method used as a diagnostic indicator.

3.2 Influence of Harmonic Voltages on the Neutral Current Method

3.2.1 Harmonic Components of Neutral Currents of Aged and Unaged MOSA Under Pure Sinusoidal Applied Voltage

Before the influence of harmonic voltages on the neutral current method can be investigated, the harmonic components of the neutral current under pure sinusoidal applied voltage should be found and used as a reference. Here, software PSCAD/EMTDC$^+$ is used to simulate the MOSA valve elements in the three-phase configuration.

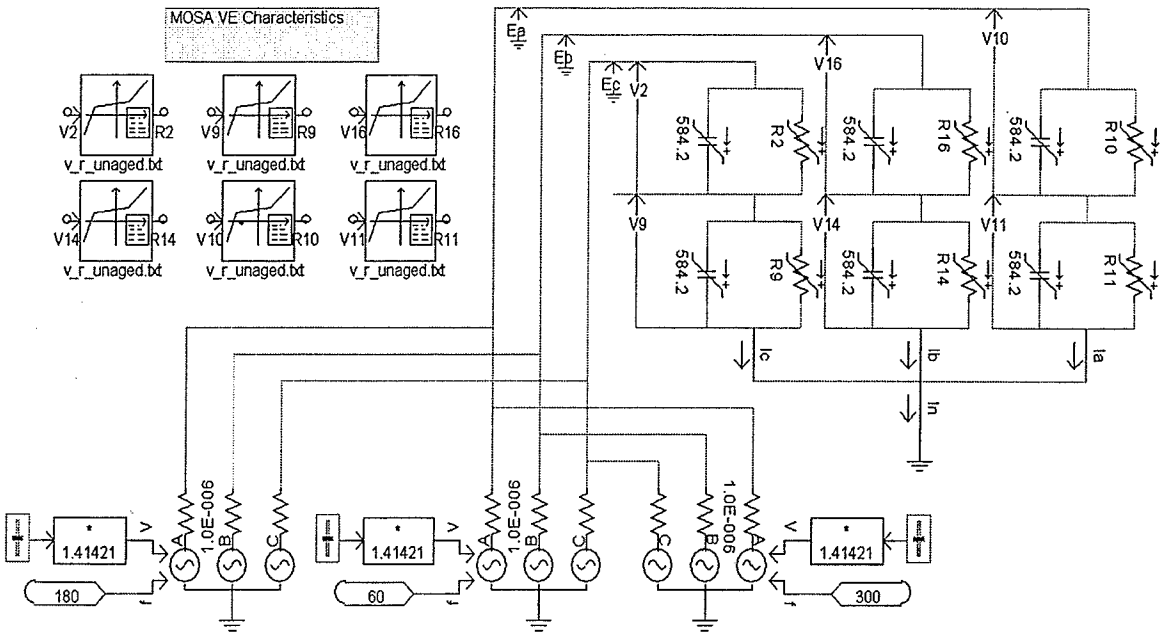

Fig. 3.2 PSCAD simulation to evaluate effect of harmonics in applied voltage

Fig. 3.2 shows a PSCAD case used in this simulation. Each MOSA valve element is represented by a capacitor in parallel with a nonlinear resistor as discussed in Chapter 2. The value of the capacitor varies with applied voltage as well but, since it is not significant it was assumed to be constant at a value of 584.2pF for unaged MOSA valve elements. The section labeled "MOSA VE Characteristics" includes data files that determine the nonlinear resistance of the valve elements. The data file labeled as v_r_unaged.txt is created to represent the voltage and resistance in a data file according to the derived polynomial representation of v-i_r characteristics mentioned in Chapter 2. In the data file, the voltage step is 0.01 p.u.. If voltage and resistive current are known, the nonlinear resistance of the valve element is the ratio between the instantaneous values of voltage and current. By changing the text file, the characteristics of the individual valve

element can be changed.

Two cases were considered. In the first case (section 3.2.1.1) identical unaged valve elements, which have the same characteristics as shown in Chapter 2 (page 23 V.E #9), are present in all phases. In the second case (section 3.2.1.2) one valve element (#4) in phase C is aged. In both cases the applied voltage was equal to 11kV RMS.

3.2.1.1 Pure Sinusoidal Applied Voltage: Unaged Valve Elements in all three phases

Fig. 3.3 shows the three phase currents (I_a, I_b, I_c), the phase A current, the neutral current and the phase A voltage. It is seen that the neutral current waveform is of a rather uniform third harmonic. Each peak value of the neutral current is 0.4538mA.

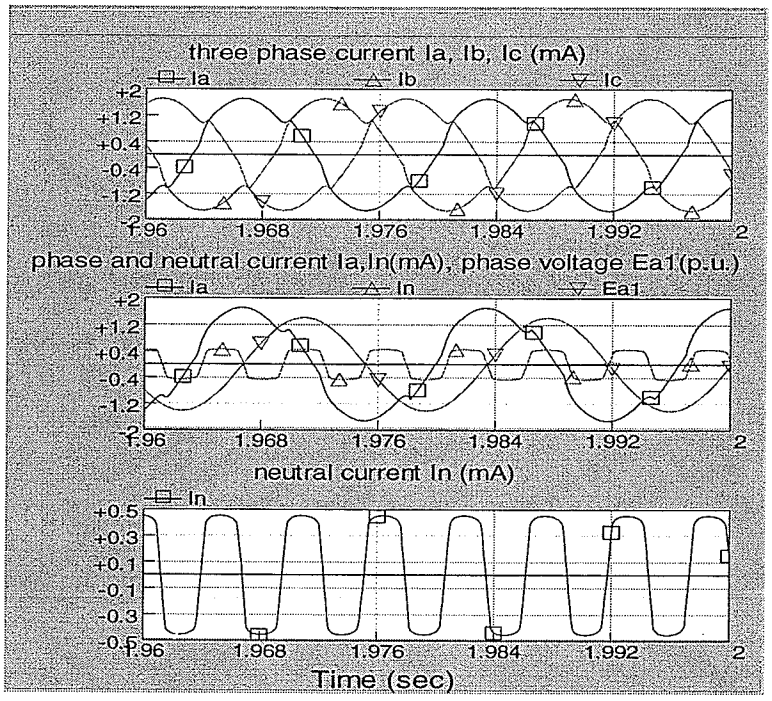

Fig. 3.3 PSCAD simulation results: unaged valve elements in all phases, 11kV RMS sinusoidal applied voltage

Fig 3.4 shows the frequency spectrum of the neutral current obtained by use of the LiveWire software. From Fig. 3.4 it can be seen that the neutral current, due to the presence of unaged MOSA valve elements in the three phases, mainly contains the 3rd, 9th and 15th harmonics. The third harmonic component is the largest. If we regard 180Hz as the fundamental, the harmonic components in the neutral current gradually decreases with increase in the harmonic order.

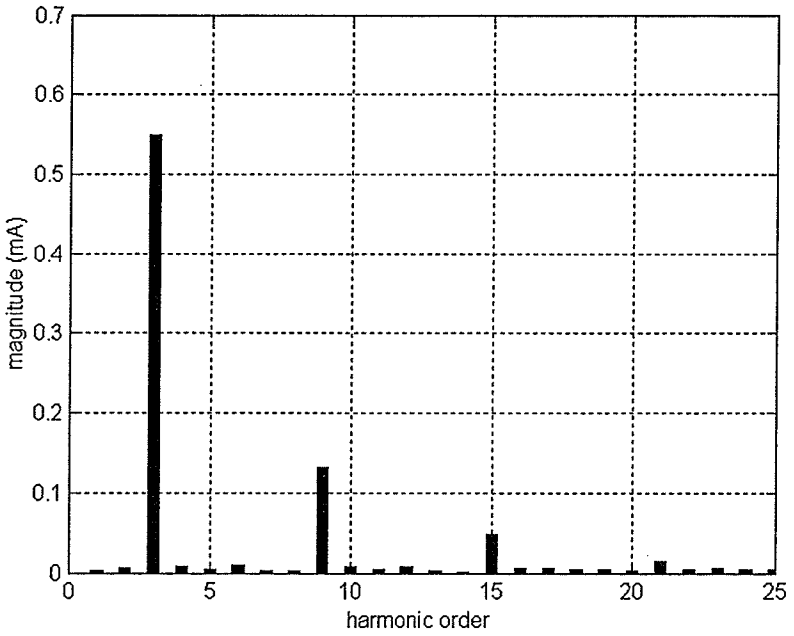

Fig. 3.4 Spectrum of the neutral current with unaged valve elements in all phases, 11kV RMS sinusoidal applied voltage

3.2.1.2 Pure Sinusoidal Applied Voltage: One Aged Valve Element in Phase C

The capacitance of the aged MOSA valve element is 636.1pF, which was calculated by the compensation method mentioned in Chapter 2. The resistance of the aged MOSA

valve element varies with instantaneous applied voltage and a data file for aged elements represents its nonlinear characteristic. Fig. 3.5 shows the neutral current, total current per phase and the applied voltage waveforms for this case. The neutral current peak values within one cycle of phase A voltage are 0.3873mA, 0.5145mA and 0.9422mA respectively.

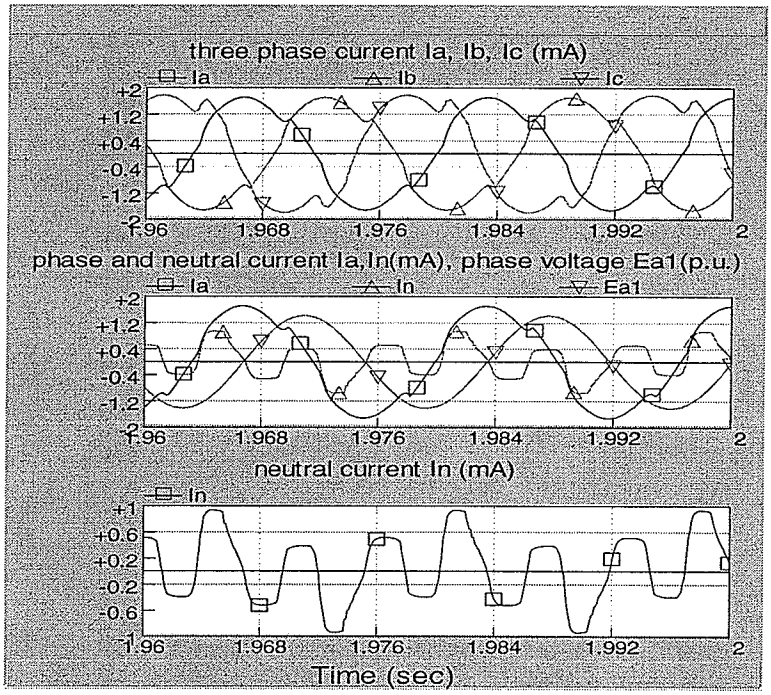

Fig. 3.5 PSCAD simulation results: One aged valve element in phase C (#4), 11kV RMS sinusoidal applied voltage

Fig 3.6 shows the frequency spectrum of the neutral current for aged simulation case. Comparing Fig. 3.6 with Fig. 3.4, it can be seen that the neutral current in this case has more harmonic components and of higher magnitudes. The distortion of the neutral current waveform is serious. The third harmonic (180Hz) component is still the largest harmonic.

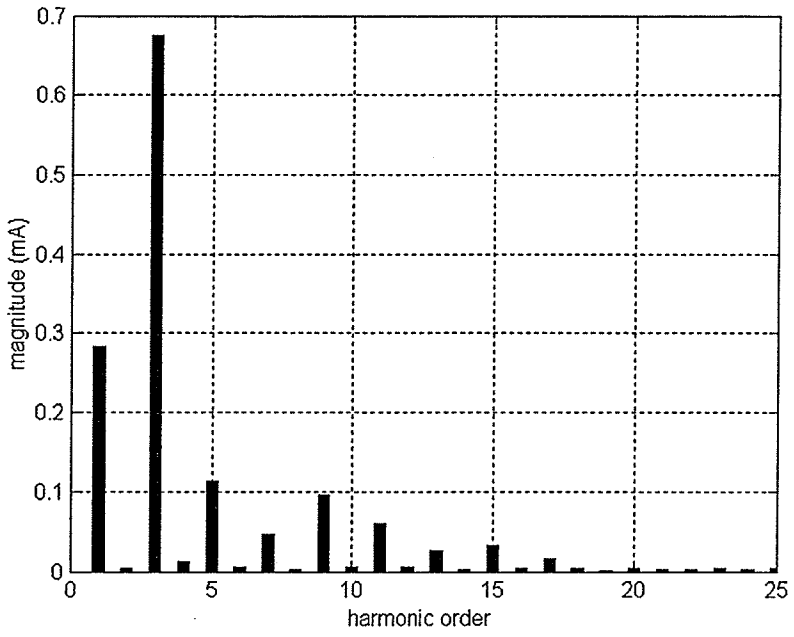

Fig. 3.6 Spectrum of the neutral current with one aged valve element in phase C, 11kV RMS sinusoidal applied voltage

3.2.2 Harmonic Content of Voltage in Power Systems

In a power system, harmonic voltages can be introduced at the generator end and in transmission and distribution systems because of unbalanced faults, non-linear excitation of power transformers, and increased use of power electronic devices. Even the synchronous generator itself injects harmonic voltage contents into a power system. At the customer end, the use of arc furnaces in iron-steel industries, TV sets, fluorescent lighting installations and the increasing use of Pulse Width Modulation (PWM) drives for ac motors, etc, are very common. All these loads will result in the introduction of harmonic currents into the power system and will cause the further distortion of the bus

voltage which is connected with such loads [14].

The spread of harmonic currents in a power system depends on the power system configuration and results in a very complicated harmonic voltage distribution pattern. The harmonic content will be rather different in different portions of the same power system such as low voltage system, medium voltage system, and so on. Furthermore, the harmonic components and their magnitudes in a power system will vary with time. The same can be said for the phase angles of the harmonic components. Therefore, in practice, the voltage across a MOSA in service will never be a pure sinusoid. The harmonic distortion of the applied voltage might affect the wave shape and the harmonic spectrum of the neutral current. This aspect is investigated in the following section.

3.2.3 Effect of Harmonic Voltages on the Neutral Current Method

As discussed above, the harmonic components in the voltage will never be constant. In the following simulation, the effects of the 3^{rd} and 5^{th} harmonic components acting alone and in various combinations are discussed.

The magnitude of the 3^{rd} harmonic voltage component and its phase angle are designated by V_3 and Φ_3 respectively. In a similar way, the magnitude of the 5^{th} harmonic voltage component and its phase angle are designated by V_5 and Φ_5 respectively. The actual voltage across the MOSA is obtained by addition of the fundamental and the 3^{rd}, 5^{th} harmonic voltage components.

$$v = V_1 \cos(\omega t) + V_3 \cos(3\omega t + \Phi_3) + V_5 \cos(5\omega t + \Phi_5) \quad (3\text{-}1)$$

Using PSCAD, both unaged and aged cases were examined. These cases are the same as those considered in section 3.2.1 (page 50). The influence of harmonic voltages on the neutral current waveforms and frequency spectrum of the neutral current was investigated for applied voltages with the following harmonic contents.

Case1: V_3=0, V_5=0

Case2: Φ_3=0°, V_3=3%V_1

Case3: Φ_3=180°, V_3=3%V_1

Case4: Φ_5=0°, V_5=3%V_1

Case5: Φ_5=180°, V_5=3%V_1

Case6: Φ_3=0°, V_3=3%V_1, Φ_5=0°, V_5=3%V_1

Case7: Φ_3=180°, V_3=3%V_1, Φ_5=0°, V_5=3%V_1

Case8: Φ_3=0°, V_3=3%V_1, Φ_5=180°, V_5=3%V_1

Case9: Φ_3=180°, V_3=3%V_1, Φ_5=180°, V_5=3%V_1

It may be mentioned that according to the IEEE Std 519-1992 [15], as shown in Table 3.2, the maximum allowed individual voltage distortion is 3% for voltages less than or equal to 69 kV.

Table 3.2 Voltage Distortion Limits [15]

Bus Voltage at PCC	Individual Voltage Distortion (%)	Total Voltage Distortion THD (%)
69 kV and below	3.0	5.0
69.001 kV through 161 kV	1.5	2.5
161.001 kV and above	1.0	1.5

3.2.3.1 Effect of Harmonic Voltage on Spectral Components of the Neutral Current

As the harmonic components of 180Hz, 540Hz and 900Hz are primary, we focus on comparison of these harmonic contents. Table 3.3 shows harmonic contents of the neutral current obtained from the various simulations.

Table 3.3 Comparison of the Neutral Current Harmonic Content for applied voltages with differing harmonic contents (maximum 3% content)

Case Number		Harmonic Component of Voltage (%)		Phase Angle (°)		In_{180Hz} (mA)	In_{540Hz} (mA)	In_{900Hz} (mA)	In_{540Hz}/In_{180Hz} (%)	In_{900Hz}/In_{180Hz} (%)
		V_3	V_5	Φ_3	Φ_5					
unaged valve elements in all phases	#1	0	0	0	0	0.550	0.132	0.049	24	8.91
	#2	3	0	0	0	0.545	0.121	0.038	22.20	6.98
	#3	3	0	180	0	0.545	0.119	0.038	21.83	6.97
	#4	0	3	0	0	0.545	0.121	0.038	22.13	6.99
	#5	0	3	0	180	0.545	0.120	0.038	21.99	7.06
	#6	3	3	0	0	0.535	0.098	0.017	18.39	3.14
	#7	3	3	180	0	0.547	0.125	0.044	22.87	8.00
	#8	3	3	0	180	0.547	0.125	0.043	22.87	7.92
	#9	3	3	180	180	0.534	0.099	0.029	18.48	5.49
one aged valve element in phase C	#1	0	0	0	0	0.675	0.096	0.033	14.22	4.89
	#2	3	0	0	0	0.704	0.096	0.024	13.64	3.41
	#3	3	0	180	0	0.633	0.098	0.017	15.48	2.69
	#4	0	3	0	0	0.663	0.094	0.015	14.18	2.26
	#5	0	3	0	180	0.674	0.094	0.043	14.01	6.32
	#6	3	3	0	0	0.699	0.086	0.011	12.34	1.63
	#7	3	3	180	0	0.699	0.086	0.011	12.34	1.63
	#8	3	3	0	180	0.702	0.096	0.039	13.71	5.51
	#9	3	3	180	180	0.638	0.090	0.035	14.17	5.50

From Table 3.3 it can be seen that harmonics present in the applied voltage definitely

influence the harmonic components in the neutral current especially when an aged valve element is present in one of the phases. For example, the 180Hz harmonic content of the neutral current for the unaged case changes only slightly from 0.534mA to 0.550mA, whereas the 180Hz harmonic content of the neutral current for the aged case varies in the range from 0.633mA to 0.704mA.

Of primary concern is the magnitude of the neutral current peak since they are used in the program logic to find out the condition of the arresters.

3.2.3.2 Effect of Harmonics in Applied Voltage on the Three Peak Values of the Neutral Current

For each case, the three peak values of the neutral current and the waveshape factors were calculated to check if the harmonic components present in the applied voltage introduce any error in the neutral current used as a diagnostic indicator. The simulated and calculated results are shown in Table 3.4.

It may be recalled that the criteria for classification of valve element condition is based on the value of waveshape factor k ($k_x \leq 2$, phase x is unaged; $2 < k_x < 5$, phase x is aged; $k_x \geq 5$, phase x is damaged). Comparing the waveshape factors for the aged and unaged cases in Table 3.4, it is seen that in spite of the presence of harmonics (maximum 3% content) the classification of valve element condition is not affected.

Table 3.4 Comparison of three peak values of Various Cases, maximum 3% harmonic content

Case Number		Harmonic component of Voltage (%)		Phase Angle (°)		Three Peak Values (mA)			Waveshape Factors		
		V_3	V_5	Φ_3	Φ_5	Peak1	Peak2	Peak3	k_1	k_2	k_3
unaged valve elements in all phases	#1	0	0	0	0	0.4538	0.4538	0.4538	1	1	1
	#2	3	0	0	0	0.4411	0.4628	0.4625	1	1.05	1.05
	#3	3	0	180	0	0.4657	0.4494	0.4493	1.04	1.00	1
	#4	0	3	0	0	0.4684	0.4525	0.4527	1.04	1	1.00
	#5	0	3	0	180	0.441	0.4643	0.4642	1	1.05	1.03
	#6	3	3	0	0	0.4546	0.4641	0.4643	1	1.02	1.02
	#7	3	3	180	0	0.4797	0.4421	0.4421	1.09	1	1
	#8	3	3	0	180	0.4274	0.4687	0.4688	1	1.10	1.10
	#9	3	3	180	180	0.4548	0.4617	0.4616	1	1.02	1.01
one aged valve element in phase C	#1	0	0	0	0	0.3873	0.5145	0.9422	1	1.33	2.44
	#2	3	0	0	0	0.3845	0.53	0.954	1	1.38	2.48
	#3	3	0	180	0	0.4014	0.5125	0.9302	1	1.28	2.32
	#4	0	3	0	0	0.3989	0.5161	0.9078	1	1.29	2.28
	#5	0	3	0	180	0.3874	0.5374	0.9705	1	1.39	2.51
	#6	3	3	0	0	0.3903	0.5328	0.9416	1	1.37	2.42
	#7	3	3	180	0	0.4073	0.4998	0.8962	1	1.23	2.20
	#8	3	3	0	180	0.3794	0.5428	0.9795	1	1.43	2.58
	#9	3	3	180	180	0.3958	0.5352	0.9633	1	1.35	2.43

According to IEEE Std 519-1992 a maximum individual voltage distortion of 4.5% is allowed for short periods [15]. Therefore, the effect of harmonics is also considered for harmonic contents of 4.5%. Cases 10 to 17 are similar to cases 1 to 9 with the exception that the harmonic content is 4.5%. The results are presented in Table 3.5 and Table 3.6.

Table 3.5 Comparison of Neutral Current Harmonic Content for applied voltages with differing harmonic contents (maximum 4.5% content)

Case Number		Harmonic Component of Voltage (%)		Phase Angle (°)		In_{180Hz} (mA)	In_{540Hz} (mA)	In_{900Hz} (mA)	In_{540Hz}/In_{180Hz} (%)	In_{900Hz}/In_{180Hz} (%)
		V_3	V_5	Φ_3	Φ_5					
unaged valve elements in all phases	#1	0	0	0	0	0.550	0.132	0.049	24	8.91
	#10	4.5	0	0	0	0.540	0.109	0.026	20.21	4.89
	#11	4.5	0	180	0	0.537	0.104	0.028	19.36	5.24
	#12	0	4.5	0	0	0.538	0.106	0.027	19.66	4.95
	#13	0	4.5	0	180	0.539	0.107	0.029	19.85	5.30
	#14	4.5	4.5	0	0	0.520	0.068	0.003	13.10	0.63
	#15	4.5	4.5	180	0	0.542	0.116	0.038	21.37	6.97
	#16	4.5	4.5	0	180	0.531	0.124	0.032	23.42	6.06
	#17	4.5	4.5	180	180	0.518	0.074	0.025	14.32	4.90
one aged valve element in phase C	#1	0	0	0	0	0.675	0.096	0.033	14.22	4.89
	#10	4.5	0	0	0	0.714	0.100	0.020	14.05	2.77
	#11	4.5	0	180	0	0.610	0.090	0.006	14.83	1.04
	#12	0	4.5	0	0	0.656	0.075	0.004	11.48	0.58
	#13	0	4.5	0	180	0.671	0.089	0.042	13.23	6.31
	#14	4.5	4.5	0	0	0.698	0.080	0.037	11.41	5.35
	#15	4.5	4.5	180	0	0.583	0.064	0.019	10.98	3.21
	#16	4.5	4.5	0	180	0.697	0.100	0.029	14.35	4.16
	#17	4.5	4.5	180	180	0.620	0.0778	0.040	12.54	6.38

Table 3.6 Comparison of three peak values of various cases, maximum 4.5% harmonic content

Case Number		Harmonic component of Voltage (%)		Phase Angle (°)		Three Peak Values (mA)			Waveshape Factors		
		V_3	V_5	Φ_3	Φ_5	Peak1	Peak2	Peak3	k_1	k_2	k_3
unaged valve elements in all phases	#1	0	0	0	0	0.4538	0.4538	0.4538	1	1	1
	#10	4.5	0	0	0	0.4342	0.4673	0.4676	1	1.08	1.08
	#11	4.5	0	180	0	0.4751	0.4481	0.4481	1.02	1	1
	#12	0	4.5	0	0	0.4751	0.4547	0.4598	1.04	1	1.01
	#13	0	4.5	0	180	0.4345	0.47	0.4698	1	1.08	1.08
	#14	4.5	4.5	0	0	0.4548	0.4698	0.4737	1	1.03	1.04
	#15	4.5	4.5	180	0	0.4956	0.4372	0.4373	1.13	1	1.00
	#16	4.5	4.5	0	180	0.4195	0.4761	0.4758	1	1.13	1.13
	#17	4.5	4.5	180	180	0.4547	0.4679	0.4678	1	1.03	1.03
one aged valve element in phase C	#1	0	0	0	0	0.3873	0.5145	0.9422	1	1.33	2.44
	#10	4.5	0	0	0	0.3802	0.5364	0.9644	1	1.41	2.54
	#11	4.5	0	180	0	0.4056	0.5118	0.9294	1	1.26	2.29
	#12	0	4.5	0	0	0.4017	0.5197	0.8627	1	1.29	2.15
	#13	0	4.5	0	180	0.3854	0.5482	0.9848	1	1.42	2.56
	#14	4.5	4.5	0	0	0.389	0.5445	0.9614	1	1.40	2.47
	#15	4.5	4.5	180	0	0.4144	0.4951	0.8689	1	1.19	2.10
	#16	4.5	4.5	0	180	0.3743	0.555	0.9992	1	1.48	2.67
	#17	4.5	4.5	180	180	0.3973	0.5469	0.9773	1	1.38	2.46

Tables 3.5 and 3.6 indicate the same conclusion as Tables 3.3 and 3.4, which is that the harmonics present in the applied voltage definitely influence the harmonic components in the neutral current but the classification of valve element condition is not affected.

3.2.3.3 Summary of the Influence of Harmonic Voltage

In conclusion, the harmonics present in the applied voltage do affect the frequency spectrum of the neutral current, but do not influence the diagnostic ability of the neutral current method. The neutral current method, in contrast with other methods based on harmonic analysis, is particularly insensitive to the influence of the harmonics in power systems.

3.3 Influence of Unbalanced Phase Voltage on the Neutral Current Method

According to operational experience of Manitoba Hydro, the voltage of 66kV system with delta connection is well balanced. Unbalance usually occurs in 25kV or lower systems with a star connection. The worst unbalance value is 10 percent at the station. Therefore, a reasonable unbalance value to be used in the simulation is 10 percent. The influence of increase or decrease in a phase voltage by 10 percent is therefore examined. From sections 3.2.1.1 and 3.2.1.2, it may be recalled that the three peak values of the neutral current with identical unaged MOSA valve elements in all three phases is 0.4538mA under balanced pure sinusoidal voltage. The three peak values of the neutral current and waveshape factors obtained with one aged MOSA valve element (#4) in phase C under balanced voltage without harmonics are shown in Table 3.7. Here, Peaks 1, 2, 3 correspond to phases A, B and C respectively.

Table 3.7 Three peak values of the neutral current and waveshape factors with one aged MOSA valve element in phase C, balanced sinusoidal applied voltage 11kV

Peak Value (mA)	Peak1=0.3873	Peak2=0.5145	Peak3=0.9422
Waveshape Factor	k_1=1	k_2=1.328	k_3=2.433

3.3.1 Effect of Increase in Phase A Voltage by 10 Percent

Fig. 3.7 shows the relationship of the three phase voltages when the voltage in phase A is increased by 10 percent.

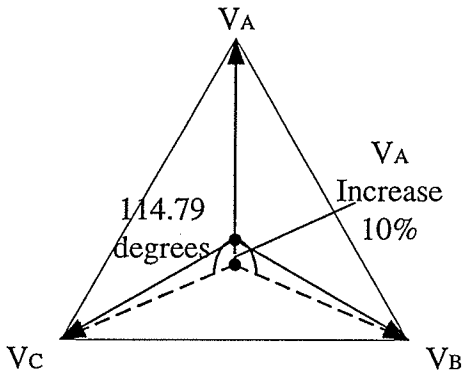

Fig. 3.7 Relationship of the three phase voltages with increase in phase A voltage by 10%

Since, in our simulation, the system rated phase voltage is 11kV, the values of the phase B and phase C voltages may be found to be 10.4933kV (RMS). There is also an accompanying phase shift which is identified in Fig. 3.7. The following MOSA cases are simulated under this condition of unbalance.

3.3.1.1 Identical Unaged MOSA in All Three Phases

With identical unaged MOSA valve elements in all three phases and unbalanced

phase voltages as defined in section 3.3.1, the three peak values of the neutral current and the waveshape factors obtained by simulation are shown in Table 3.8.

Table 3.8 Three peak values of the neutral current and waveshape factors with identical unaged valve elements in all three phases, increase in phase A voltage by 10 percent

Peak Value (mA)	Peak1=0.6732	Peak2=0.0199	Peak3=0.9218
Wave-shape Factor	k_1=33.83	k_2=1	k_3=46.32

Comparing the entries of Table 3.8 with the peak values of the neutral current with identical unaged MOSA valve elements in all three phases under balanced pure sinusoidal voltage (0.4538 mA, section 3.3), it can be noticed that the values of peak1 and peak3 are increased while peak2 value is decreased. Table 3.8 shows that the waveshape factors give rise to a wrong conclusion that valve elements in phases A and C are both damaged.

3.3.1.2 One Aged MOSA Valve Element in Phase B

One of the two valve elements in phase B is assumed to be aged (V.E #4). All remaining valve elements are unaged and identical. The three peak values of the neutral current and waveshape factors obtained are shown in Table 3.9.

Table 3.9 Three peak values of the neutral current and waveshape factors with one aged valve element in phase B, increase in phase A voltage by 10 percent

Peak Value (mA)	Peak1=0.6926	Peak2=0.4058	Peak3=0.8671
Wave-shape Factor	k_1=1.71	k_2=1	k_3=2.14

From Table 3.9 it can be concluded that phase C is defective while phases A and B are both unaged. This mistaken indication is the result of a decrease in the value of peak corresponding to the defective phase due to the unbalanced applied voltage.

3.3.1.3 One Aged MOSA Valve Element in Phase C

The simulation results obtained after switching the aged MOSA valve element from phase B to phase C are shown in Table 3.10.

Table 3.10 Three peak values of the neutral current and waveshape factors with one aged valve element in phase C, increase in phase A voltage by 10 percent

Peak Value (mA)	Peak1=0.6038	Peak2=0.0964	Peak3=1.3179
Wave-shape Factor	k_1=6.26	k_2=1	k_3=13.67

The wave-shape factors indicate that the valve element in phases A and C are damaged. This identification result is incorrect.

3.3.1.4 Summary of the Influence of Unbalanced Voltage Due to Increase in Phase A Voltage

The influence of unbalanced voltage due to increase in phase A voltage is quite serious. Although unaged MOSA valve elements may be present in all three phases, one obtains a wrong indication that the valve elements in two of the three phases are damaged.

If the valve elements in one phase are aged and in phase B, incorrect diagnostic results may be obtained once again, which indicate that elements in phase C are aged while phase B is unaged. In this case the aged valve element is situated in the phase associated with decrease in the voltage i.e. phase B.

If one aged valve element is situated in phase C, one can obtain the incorrect phase identification of phase A.

3.3.2 Effect of Decrease in Phase A Voltage by 10 Percent

Fig. 3.8 shows the relationship of the three phase voltages when the voltage in phase A is decreased by 10 percent.

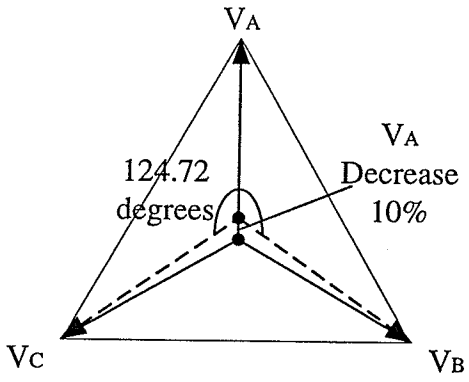

Fig.3.8 Relationship of the three phase voltages with decrease in phase A voltage by 10%

The values of the phase B and phase C voltages may be found to be equal to 11.5892kV (RMS). There is also an accompanying phase shift which is identified in Fig. 3.8. The following MOSA cases are simulated under this condition of unbalance.

3.3.2.1 Identical Unaged MOSA in All Three Phases

With identical unaged MOSA valve elements in all three phases and unbalanced phase voltages as defined in section 3.3.2, the three peak values of the neutral current and the waveshape factors are shown in Table 3.11.

Table 3.11 Three peak values of the neutral current and waveshape factors with identical unaged valve elements in all three phases, decrease in phase A voltage by 10 percent

Peak Value (mA)	Peak1=0.3652	Peak2=0.9485	Peak3=0.1585
Wave-shape Factor	k_1=2.30	k_2=5.98	k_3=1

Comparing Table 3.11 with the peak values of the neutral current with identical unaged MOSA valve elements in three phases under balanced pure sinusoidal voltage, it can be seen that the values of peak1 and peak3 are decreased whereas peak2 value is increased. The Table 3.11 shows that the waveshape factors give rise to a wrong conclusion that valve elements in phases A and B are defective.

3.3.2.2 One Aged MOSA Valve Element in Phase B

One of the two valve elements in phase B is assumed to be aged (V.E. #4). All remaining valve elements are unaged and identical. The three peak values of the neutral current and waveshape factors obtained are shown in Table 3.12.

Table 3.12 Three peak values of the neutral current and waveshape factors for with aged valve element in phase B, decrease in phase A voltage by 10 percent

Peak Value (mA)	Peak1=0.4345	Peak2=1.4736	Peak3=0.0825
Wave-shape Factor	k_1=5.27	k_2=17.86	k_3=1

The waveshape factors indicate that phases A and B are defective. This identification result of phase A is incorrect.

3.3.2.3 One Aged MOSA Valve Element in Phase C

The simulation results obtained after switching the aged MOSA valve element from phase B to phase C are shown in Table 3.13.

Table 3.13 Three peak values of the neutral current and waveshape factors with one aged valve element in phase C, decrease in phase A voltage by 10 percent

Peak Value (mA)	Peak1=0.3072	Peak2=1.0096	Peak3=0.1804
Wave-shape Factor	k_1=1.70	k_2=5.60	k_3=1

The diagnostic result of the neutral current method is that valve element in phase B is damaged while phase C is unaged. This mistaken identification about phase B is the result of an increase in the value of peak2 due to the unbalanced voltage.

3.3.2.4 Summary of the Influence of Unbalanced Voltage Due to Decrease in Phase A Voltage

The unbalanced voltage due to decrease in phase A voltage has a strong influence on the diagnostics provided by the neutral current method with identical unaged MOSA elements in all three phases. One may obtain a wrong identification that the valve elements in two of three phases are defective.

If the valve elements in one phase are aged and in phase B, the incorrect phase identification can be obtained again.

If one aged valve element is situated in phase C, incorrect diagnostic results may be obtained once again, which indicates that element in phase B is aged while phase C is unaged. In this case the aged element is situated in the phase associated with increase in the voltage i.e. phase B.

3.3.3 Effect of Increase And Decrease in Phase A Voltage by 3 Percent

With grounded neutral system unbalance of 3% or less may be expected. Analysis similar to that discussed in section 3.3.1 and 3.3.2 was come out with an unbalance of 3%. With an unbalance of 3% in phase A voltage, the phase shift may be 118.49° and 121.47° instead of 114.79° and 124.72°. The results are shown in Table 3.14.

Table 3.14 Simulation results of increase and decrease in phase A voltage by 3%

Unbalance	Phase A	Phase B	Phase C	Waveshape Factors		
				k_1	k_2	k_3
increase in phase A voltage by 3%	unaged	unaged	unaged	1.54	1	1.84
	unaged	aged	unaged	1.02	1.46	1
	unaged	unaged	aged	1.09	1	2.71
decrease in phase A voltage by 3%	unaged	unaged	unaged	1.36	1.76	1
	unaged	aged	unaged	1.98	4.08	1
	unaged	unaged	aged	1	1.66	2.12

From Table 3.14 it can be noticed that if one aged valve element is in phase B identification result obtained is that all three phases are unaged. This is incorrect due to increase in phase A voltage by 3%.

CHAPTER 4

Conclusions

4.1 Summary

In this thesis, the applicability of the neutral current method used as an on-site diagnostic technique for assessing the condition of MOSA is investigated. Furthermore, the effects of voltage harmonics, unbalanced voltage and inter-phase interference on the diagnostic indicator are studied.

In Chapter 2, the v-i_r characteristics of some aged and unaged MOSA valve elements used in the experiments are derived by application of the compensation method. The representation of simplified v-i_r characteristic curves of MOSA valve element in the low electric field region is obtained. Secondly, experimental data is presented obtained by application of the neutral current diagnostic method in a laboratory setting using a three-phase setup for various cases employing combinations of aged and unaged valve elements. Finally, a LabVIEW program has been developed to enable phase identification of aged element or elements by using the neutral current method. Installation of the LabVIEW program in a laptop computer in conjunction with suitable

current monitors ensures the portability of this diagnostic method.

In Chapter 3, the influence of inter-phase on the neutral current as a diagnostic indicator of MOSA in service is experimentally investigated. The effects of harmonics present in the applied voltage and unbalanced phase voltage are also investigated in this chapter by using PSCAD/EMTDC^{+}.

4.2 Conclusions

The following conclusions may be drawn from the study in this thesis:

(1) The neutral current method, with its simplicity and convenience of use, can be used to quickly assess the condition of MOSA per phase in service.

(2) The instrumentation required with the neutral current technique is easily portable and can be used by non-specialists to quickly assess the condition of arresters and decide whether or not a more detailed investigation is required.

(3) Inter-phase interference has negligible influence on the neutral current method used as a diagnostic technique of MOSA valve elements in service.

(4) Harmonics present in the applied voltage affect the frequency spectrum of the neutral current, but do not influence the neutral current used as a diagnostic indicator.

(5) Unbalanced voltage can introduce errors in the diagnosis provided by the

neutral current which results in incorrect identification of aged MOSA.

4.3 Recommendations for Future Research

This thesis offers the following suggestions for future work:

(1) The criteria used by LabVIEW program to classify the condition of the MOSA valve elements may be modified by taking into account field experience.

(2) The neutral current method as proposed in this thesis should be implemented in the field and results obtained compared with that obtained by other field and laboratory methods.

(3) The influence of the temperature of surroundings on diagnosis needs to be considered.

(4) By examination of the symmetry of one current in one phase a judgment can be made about the type and value of impulses to which this one has been suggested [16].

REFERENCES

[1] T. Klein, W. Köhler, K. Feser, W. Schmidt, R. Bebensee, "A New Monitoring System for Metal Oxide Surge Arresters", High Voltage Engineering Symposium, Vol. 2, 22-27 August 1999, pp 301-304

[2] M. de Nigris, A. Sironi, I. Bonfanti, F. Giornelli, C. Valagussa, Li Kaishing, "Most Recent Developments in Surge Arresters Technology and Testing", International Conference on Power System Technology, Vol. 1, 18-21 August 1998, pp 194 -201

[3] E. C. Sakshaug, "A Brief History of AC Surge Arresters", IEEE Power Engineering Review, Vol. 11, August 1991, pp 11 -13, 40

[4] A. Schei, K. H. Weck, "Metal Oxide Surge Arrester in AC Systems Part 1: General Properties of the Metal Oxide Surge Arrester", Electra, N° 128, 1990, pp. 100-105

[5] C. Heinrich, V. Hinrichsen, "Diagnostics and Monitoring of Metal-Oxide Surge Arresters in High-Voltage Networks—Comparison of Existing and Newly Developed Procedures", IEEE Trans. Power Delivery, Vol. 16, No. 1, January 2001, pp 138-143

[6] J. C. Montenegro, J. L. Ramirez, "Degradation of Zinc Oxide Varistors", Proceedings of IEEE International Caracas Conference on Circuits and Systems, 12-14 December 1995, pp 352 -354

[7] Hanxin Zhu, "Investigation of On-site Diagnostic Testing of Metal Oxide Surge Arresters", M. Sc. Thesis, University of Manitoba, April 2000

[8] Hanxin Zhu, M. R. Raghuveer, "Influence of Harmonics in System Voltage on Metal Oxide Surge Arrester Diagnostics", Conference on Electrical Insulation and Dielectric Phenomena, Vol. 2, 1999, pp 542 -545

[9] S. N. Fernando, M. R. Raghuveer, "Technique to Examine the Influence of Voltage Harmonics on Leakage Current Based MOSA Diagnostic Indicator", CEIDP, Vol.2 2000, pp 596 -599

[10] J. Lunquist, L. Stenstrom, A. Schei, B. Hansen, "New Method for Measurement of the Resistive Leakage Current of Metal-Oxide Surge Arresters in Service", IEEE Trans. Power Delivery, Vol.5, No.4, November 1990, pp 1811-1822

[11] V. Hinrichsen, G. Scholl, M. Schubert, T. Ostertag, "Online Monitoring of High-Voltage Metal-Oxide Surge Arresters by Wireless Passive Surface Acoustic Wave (SAW) Temperatures Sensors", in 11th ISH, London, Vol.2, August 1999, pp 238-241

[12] S. N. Fernando, "Effect of Valve Element Characteristics, Stray Capacitance and Voltage Harmonics on Surge Arrester Diagnostics", M. Sc. Thesis, University of Manitoba, June 2001

[13] W. McDermid, "Detection of Premature Aging of Gapless ZnO Arresters", Minutes of the Fifty-Fifth Annual International Conference of Doble Clients, 1988, pp 931-937

[14] J. Arrillaga, D. A. Bradley, P. S. Bodge, Electric Power Systems Harmonics, New York: Wiley c 1985

[15] IEEE Std 519-1992, "IEEE Recommended Practices and Requirements for Harmonic Control in Electrical Power Systems", Institute of Electrical and Electronics Engineers, New York, April 12, 1993

[16] M. R. Raghuveer, Xiangxiao Qiu, "Detection of Impulse Current Caused Ageing in Valve Element of A Distribution Class Metal Oxide Surge Arrester", Conference on Electrical Insulation and Dielectric Phenomena, 22-25 Oct 1995. pp 243 -246

APPENDIX

1. Tektronix TDS-3054 digital oscilloscope

Bandwidth	500 MHz
Channels	4
Sampling rate on each channel	5 GS/s
Maximum record length	10K points
Vertical resolution	9-bits
Vertical sensitivity (/div)	1 mV - 10V
Vertical accuracy	± 2%
Maximum input voltage (1MΩ)	150V RMS
Position range	± 5 div
Time base range (/div)	1 ns - 10s/div
Time base accuracy	200 ppm
Input impedance	1 MΩ in parallel with 13 pF, or 50 Ω

Optional Modules for RS-232, GPIB, LAN or VGA Communication Ports

2. Tektronix Passive High Voltage Probe P6015A

Attenuation	1000X
Bandwidth	75 MHz
Rise time	4.0 ns
Loading	100 MΩ/3pF
Maximum input voltage	20 kV RMS

3. Pearson Electronics Standard Current Monitor Model 411

Output	0.1 V/A
Maximum peak current	5,000 A

Rise time	20 ns
Approximate low frequency	1 Hz
Bandwidth	20 MHz

4. EG&G Pre-Amplifier Model 5113

Input impedance	10 MΩ or 100 MΩ in parallel with 25 pF
Maximum input voltage	DC coupled: +10V, -9V
	AC coupled: 100V
Gain	coarse gain of × 5 to × 50,000
	Fine gain of × 1 to × 100,000
Accuracy	± 1% with coarse gain, ± 2% with fine gain
Frequency response	1 MHz
Output impedance	50 Ω
Output voltage	2 V peak-peak ahead of 50 Ω

5. Data acquisition board AT-MIO-16E-2

Sampling rate	500 kS/s maximum
Resolution	12-bits
Input range	± 0.05 - ± 10 V
Output rate	1 MS/s
Output range	up to ± 10 V
Digital I/O	8
Counter/Timers	2, 24-bits

6. 5B41 voltage input module (signal conditioner)

Input voltage	-10V ~ +10V
Output voltage	-5V ~ +5V

Accuracy	± 0.05%
Bandwidth (-3dB)	10 kHz
Input resistance	650 kΩ
Input offset	± 20 μV/°C
Output offset	± 40 μV/°C
Noise	20 mV, peak-peak